Epigenetic shielding: 5-hydroxymethylcytosine and 5-carboxylcytosine modulate UV induction of DNA photoproducts

Epigenetic shielding: 5-hydroxymethylcytosine and 5-carboxylcytosine modulate UV induction of DNA photoproducts

A dissertation presented

by

Jue Judy Liu

to

The Division of Medical Sciences

in partial fulfillment of the requirements

for the degree of

Doctor of Philosophy

in the subject of

Biological Chemistry and Molecular Pharmacology

Harvard University

Cambridge, Massachusetts

February 2014

Dissertation Advisor: Professor David E. Fisher Jue Judy Liu

Epigenetic shielding: 5-hydroxymethylcytosine and 5-carboxylcytosine modulate UV induction of DNA photoproducts

Abstract

Maintaining the balance between dynamic DNA methylation and demethylation is crucial to mammalian development and pathogenesis. *In vitro* methylation at the C-5 position of cytosine enhances cyclobutane pyrimidine dimer (CPD) formation and promotes transition mutations. While the loss of 5-hydroxymethylcytosine (5hmC) and inactivation of the ten-eleven translocation (TET) family have been implicated in cancers, and repeated exposure to UV radiation is a known risk factor for developing skin cancers, the link between DNA demethylation and UV damage has not yet been illustrated. We report that hydroxylation and carboxylation of 5-methylcytosine mitigate methylation-induced CPD enhancement upon UV irradiation. However, 5hmC also increases UV induction of (6-4) photoproducts. In a melanoma cell model, this duality by 5hmC in modulating the UV response is accentuated through TET2 overexpression. These findings implicate the DNA demethylation intermediates 5-hydroxymethylcytosine (5hmC) and 5-carboxylcytosine (5caC) as selective epigenetic shields against UV induction of DNA photoproducts.

Table of Contents

List of Illustrations and Figures

Acknowledgments

First and foremost, I would like to thank my advisor, Professor David E. Fisher, for the many years of guidance, as well as the opportunity to work with him and his lab. I would also like to thank the chair of my dissertation advisory committee and of my dissertation defense committee, Professor Kristin White from the Cutaneous Biology Research Center at MGH. Many thanks go out to Professors Irene Kochevar, Anthony Letai, David Frank, Xu Wu, and Peter Dedon for their patient support and many invaluable suggestions. Deep appreciation for time and feedback also go out to Professor Yujiang Shi, Professor Roger Giese, Dr. Poguang Wang, Dr. Yinsheng Wang, Shuo Liu, Dr. Anjana Rao, Dr. Yufei Xu, Dr. Melanie Stefan, Professor Nicholas Geacintov, Professor John-Stephen Taylor, as well as my labmates Dr. Katey Robinson, Vivien Igras, Dr. Hongxiang Chen, and Jessica Fuller. Furthermore, I would like to express my sincere gratitude to Dr. David Cardozo and Dean John McNally, who have been enthusiastic supporters of the graduate student government over the years. I am also grateful to the BBS, DMS, and HILS offices.

Next, I would like to thank my family for accompanying me over the years, especially my loving husband Dr. Joseph Babcock, and my wonderful parents and in-laws.

My journey into research would not have been possible without the help from my former mentors Professor Wafik El-Deiry and Dr. Jeffrey E. Green. Last but not least, I would like to thank Harvard Medical School and the following funding institutions for supporting my research and education: The DoD, Air Force Office of Scientific Research, National Defense Science and Engineering Graduate (NDSEG) Fellowship, 32 CFR 168a; the National Cancer Institute of the National Institutes of Health under Award Number F31CA176930.

For Joseph

CHAPTER ONE: INTRODUCTION

UV Light and Skin Cancers

UV is a powerful extrinsic regulator of skin pigmentation; repetitive UV exposure can also induce skin thickening, wrinkle formation, and inflammation. Furthermore, repeated exposure to UV radiation from sunlight leads to an increased risk of developing skin cancers. UV radiation can be divided into three types: UVA (long-range UV, 320-400nm), UVB (sunburn radiation, 280-320nm), and UVC (short-wave UV, 200-280nm) (Cotton and Spandau, 1997; Paz *et al.*, 2008). UVC radiation is completely absorbed in the stratosphere by oxygen to produce ozone (Brash *et al.*, 1991), and while most of UVB light should also be absorbed before reaching the earth's surface, gradual ozone depletion has let more UVB radiation pass through the atmosphere. This trend is especially concerning, since UVB is "responsible for most of the carcinogenic effects of sun exposure" (Cotton and Spandau, 1997), and failure to eliminate UV-damaged cells through controlled apoptosis may result in disease states such as skin cancer or lead to faster aging of the skin.

Repeated exposure to UV radiation from sunlight increases the risk of developing three types of skin cancer: Malignant melanoma, basal cell carcinoma (BCC) and squamous cell carcinoma (SCC). While melanoma arises from the pigment-producing melanocytes in skin, non-melanoma skin cancers arise from keratinocytes. Squamous keratinocytes near the top of the epidermis can become cancerous, leading to squamous cell carcinoma; basal cells in the bottom layer of keratinocytes can also become cancerous, leading to basal cell carcinoma. Basal cell cancer is the most common, accounting for 80% of all skin cancers (American Cancer Society,

2008 Reference); BCC occurs most frequently (about one million new cases per year) as a hard, raised, red wound on the head, neck and other sun-exposed areas, and usually does not metastasize, but can recur. Squamous cell cancer is less common (about 200,000 new cases per year), but more aggressive and can invade nearby tissues; SCC is the most sunlight-dependent type of skin cancer, since the majority of invasive squamous cell carcinomas are marked by cytosine to thymine UVB signature mutations (Brash *et al.*, 1991). Malignant melanoma occurs even more rarely (about 50,000 new cases per year), but is the most serious type of skin cancer, usually metastasizing unless detected early (American Cancer Society, 2008 Reference; Cleaver and Crowley, 2002).

UV Lesions and DNA Mutations

When UV radiation damages a cell, it mutates the cellular DNA with distinctive mutational patterns. The major UV lesions produced are pyrimidine dimers between adjacent pyrimidines (Gale *et al.,* 1987), resulting in a four membered ring from covalent linkages of the carbon-carbon double bonds on pyrimidines (Illustration 1). These cyclobutane pyrimidine dimers (CPDs) are quite mutagenic, especially in mammalian cells, initiating primary base substitutions in DNA (Otoshi *et al.*, 2000). UV-light most dominantly induces cytosine to thymine transitions at the dipyrimidine sites, creating a UV-specific mutation signature that is ubiquitously observed in multiple organisms (Brash *et al.*, 1991). The presence of CC to TT mutations uniquely identifies UV as the mutagen, since these double base changes are exclusively due to direct UV light absorption (Brash *et al.*, 1991).

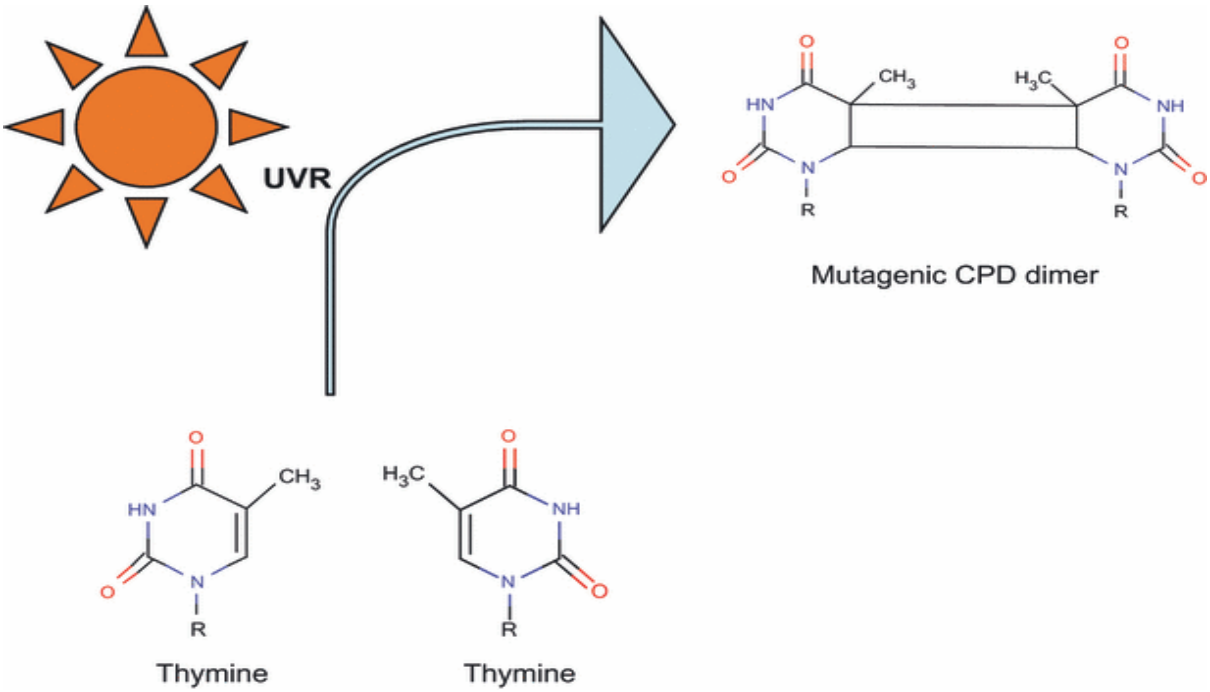

Illustration 1: TT CPD dimer formation (as published in Liu and Fisher, 2010 review)

The induction yield for CPDs depends on sequence specificity, as well as the wavelength of UV. 5' guanine inhibited CPD induction, while 3' guanine enhanced CPD induction, and CPD induction was also greater in the presence of 5' flanking pyrimidines (Cannistraro and Taylor, 2009; Mitchell *et al.*, 1991). Furthermore, the frequency of CPD formation oscillates along the core DNA, with maximum CPD formation within one base of sites where the DNA backbone is farthest from the surface of core histones, and minimum CPD formation at sites where the DNA backbone is closest to the surface of core histones (Gale *et al.*, 1987). UVB radiation produces most of the CPD photoproducts in mammalian skin compared to UVA, which comprises most of sunlight radiation at the Earth's surface; UVC is even more potent and lethal, "but it is screened out at least 10^5-fold by the ozone layer" (Brash *et al.*, 1991), and thus a minimal source of health hazards (Tran *et al.*, 2008). From *in vitro* studies of UV irradiations in plasmids, the following induction rates were observed: 2.4 CPDs per 10^8 daltons of DNA per J/m^2 UVC; 0.3 CPDs per

10^8 daltons of DNA per J/m^2 UVB (Mitchell *et al.*, 1991). While TT CPDs are the most abundant, TC or CT CPDs are more abundant than CC CPDs, with ratios ranging from 60:24:16 (UVC) to 68:29:3 (UVC), 40:40:20 (UVB) and 52:40:7 (UVB) (Mitchell *et al.*, 1991). It has been suggested that cytosine-containing dimerized pyrimidines are more mutagenic than TT dimers; since UVB induces more cytosine containing dimers, the mutational spectrum of UVB contains more deletions, insertions and C to T transition mutations at dipyrimidine sites than the mutational spectrum of UVC (Mitchell *et al.*, 1991).

The high incidence of p53 mutations at dipyrimidine sites in skin tumors correlates well with the presence of UV-induced mutagenic photoproducts (Tran *et al.*, 2008). The p53 tumor suppressor gene controls the stress and genetic-damage response pathway (Alberts *et al.*, 2002). Loss of normal p53 function not only allows abnormal cells to avoid programmed cell death, but also enables cells to accumulate additional mutations at a rapid rate by allowing abnormal cells to progress through the cell cycle and thus create many abnormal chromosomes (Alberts *et al.*, 2002). The p53 protein can be activated by a variety of stress signals, including sources that damage the integrity of the DNA template, such as gamma or UV irradiation, alkylation of bases, depurination of DNA and reaction with oxidative free radicals. In a study of patients from New England and Sweden (Brash *et al.*, 1991), 58% of invasive squamous cell carcinomas (SCC) were marked by cytosine to thymine transitions (C -> T and CC -> TT) in the p53 gene.

DNA Photoproducts

While cyclobutane pyrimidine dimers (CPDs) are responsible for the majority of UVB-induced mutations in mammalian cells, UVB and UVC can also induce (6-4) photoproducts,

another type of DNA damage formed between adjacent pyrimidine nucleotides on the same strand of DNA (Illustration 2). Both the yield and the ratio between CPDs and (6-4) photoproducts (6-4 PPs) upon UV irradiation vary greatly, depending on the chemical nature of the two pyrimidine bases involved, as well as other parameters such as the wavelength of the incident photons, the stability of the duplex DNA, and the ionic strength (Douki, 2006). The structure of the thymine-cytosine (6-4) photoproduct, the most abundant type of 6-4 PPs, was deduced by proton NMR, IR and fast atom bombardment mass spectroscopy (Franklin *et al.*, 1985). While both CPDs and 6-4 PPs are premutagenic lesions for cytosine to thymine transitions, 6-4 PPs are also premutagenic lesions for thymine to cytosine transitions (LeClerc *et al.*, 1991; Otoshi *et al.*, 2000).

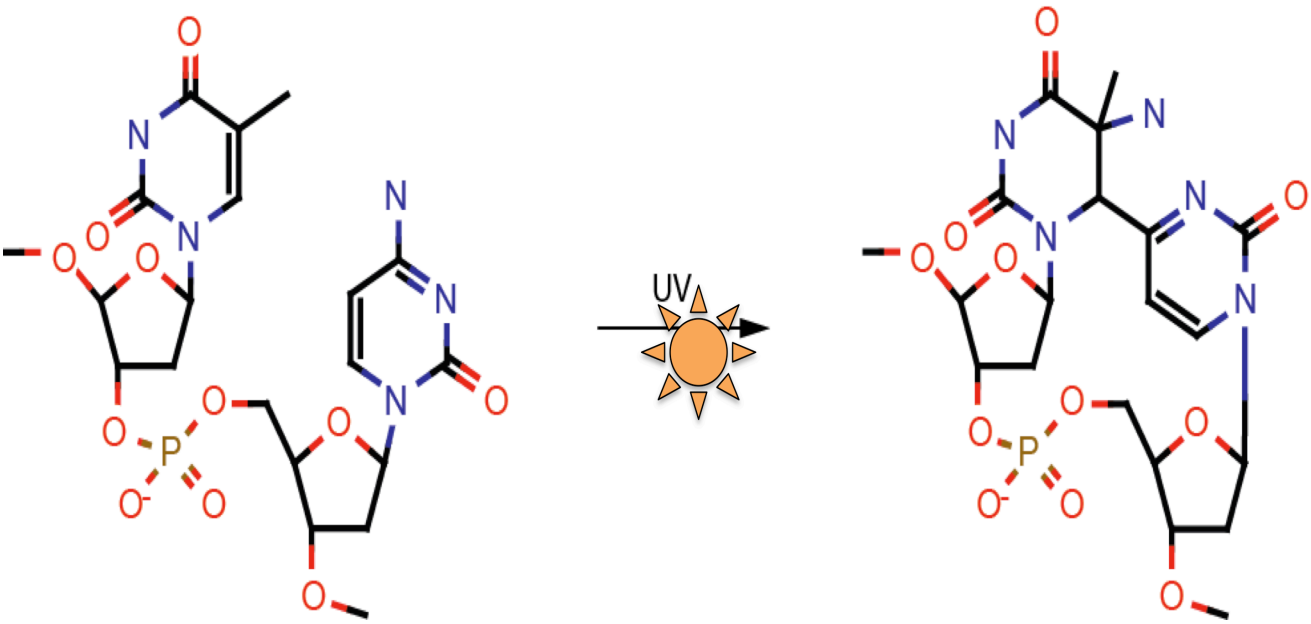

Illustration 2: TC 6-4 PP (with J. Babcock, JHU)

Under near UV irradiation around 320nm, 6-4 PPs photoisomerize to Dewar valence isomers. Two major synthesis steps are required for generating Dewar photoproduct-containing

oligonucleotides: Short oligomers with a unique thymine-thymine sequence are irradiated under UVC (254nm), upon which TT 6-4 PPs are purified by HPLC; next, these oligomers are irradiated at the longer wavelengths to produce Dewar isomers (Yamamoto *et al.*, 2006). Dewar isomers are much more unstable than 6-4 PPs (Kan *et al.*, 1992). Compared to the highly mutagenic 6-4 PPs, Dewar photoproducts also have low mutagenic potential and induce a broader range of mutations (LeClerc *et al.*, 1991; Lee *et al.*, 2000).

Epigenetic Status and UV Induction

As described above, C to T or CC to TT mutations (CPD signature mutations), have been found in the p53 gene in a large percentage of human basal and squamous cell carcinomas. Interestingly, recent technical advances have helped reveal that over a third of these p53 mutations involve 5'PymeCG trinucleotide sequences with the modified 5-methylcytosine (5meC) base (Tornaletti and Pfeifer, 1995; You and Pfeifer, 2001; Lee and Pfeifer, 2003; Cannistraro and Taylor, 2009). This correlates with observations in cultured mammalian cells that 5-methylcytosine-containing dipyrimidines are preferential targets for sunlight-induced mutagenesis (Tommasi *et al.*, 1997). One widely accepted hypothesis for the C to T transition process at dipyrimidine sequences involves the deamination of cytosine or 5-methylcytosine, followed by trans-lesion synthesis. Previous *in vitro* studies using chromatography, mass-spectrometry, enzymatic analysis, and ligation-mediated PCR have shown that methylation at the C-5 position of cytosine enhances CPD formation (under both broadband and monochromatic UVB) and promotes deamination, leading to increased UVB-induced C to T transition mutations (Douki and Cadet, 1994; Tommasi *et al.*, 1997; You *et al.*, 1999; Douki *et al.*, 2000; Mitchell,

2000; Cannistraro and Taylor, 2009; Rochette *et al.*, 2009). From a structural consideration, 5-methylcytosine enhances the dimerization reaction with the adjacent 3' end cytosine residue. Cytosine methylated at the C-5 position has a significantly lower excited singlet energy state than thymine or normal cytosine, and thus 5-methylcytosine could serve as a singlet energy trap in DNA (Tommasi *et al.*, 1997).

The "Sixth Base" and Beyond

5-methylcytosine can be converted by the TET machinery (ten-eleven translocation family of 5meC hydroxylases) into the newly (re)discovered "sixth base", 5-hydroxmethylcytosine (5hmC). The (re)discovery of 5hmC was actually an accidental finding during measurements of 5-methylcytosine: Thin-layer chromatography, high-pressure liquid chromatography, and mass spectrometry revealed an unusual DNA nucleotide, now known as 5hmC, that constitutes less than 1% of total nucleotides in neuronal cells and is not present in cancer cell lines (Kriaucionis and Heintz, 2009). The existence of 5hmC has been known in the bacteriophage world since the early 1950s (Wyatt and Cohen, 1952). The discovery of 5hmC in mammalian DNA in 2009 (Kriaucionis and Heintz, 2009; Tahiliani *et al.*, 2009) not only reawakened interest in a rare nucleotide, but also highlighted the shortcomings of previous methylation assays. In fact, enzymatic approaches and traditional bisulfite sequencing were shown to be unable to distinguish between 5meC and 5hmC in DNA (Nestor *et al.*, 2010), thus illustrating the need for urgent technical advances such as new antibodies and oxidative bisulfite sequencing (Booth *et al.*, 2012).

The TET proteins comprise a family of 2-oxoglutarate (α-ketoglutarate)- and Fe(II)-dependent enzymes (Tahiliani *et al.*, 2009). All three TET proteins contain a catalytic C-terminal CD domain (Cysteine-rich region and Double-stranded β-helix domain) (Tan and Shi, 2012). Both TET1 and TET2 regulate 5hmC production in mouse embryonic stem cells, and are induced concomitantly with 5hmC during fibroblast reprogramming into induced pluripotent stem cells (Ito *et al.*, 2010; Koh *et al.*, 2011). Disruption of TET activity was first found in myeloid tumorigenesis (Pastor *et al.*, 2011). Loss of 5hmC has recently been shown as an epigenetic hallmark of melanoma, where 5hmC and TET2 protein expression also negatively correlate with melanoma progression (Lian *et al.*, 2012; Gambichler *et al.*, 2013). In addition, 5hmC levels are decreased across a broad range of other cancers, such as oral squamous cell carcinoma (Jäwert *et al.*, 2013), brain tumors, and squamous cell lung cancers (Jin *et al.*, 2011). In an elegant experiment to show that reduced 5hmC levels are the cause and not simply the consequence of carcinogenesis, injecting TET-depleted stem cells into mice led to aggressive and proliferative tumorigenesis, while injecting wild-type stem cells into mice only led to differentiated benign teratomas (Koh *et al.*, 2011; Münzel *et al.*, 2011).

Although originally considered unlikely to be part of any active oxidative demethylation pathway due to previous inability to detect active demethylation intermediates(Globisch *et al.*, 2010), 5hmC now represents a pathway for DNA demethylation (Gong and Zhu, 2011), as it is repaired as mismatched DNA and replaced with normal cytosine. 5hmC can be further oxidized into 5-carboxylcytosine (5caC), another DNA demethylation intermediate with emerging evidence for diverse regulatory functions (Shen *et al.*, 2013; Song *et al.*, 2013; Song and He, 2013). Since the maintenance of dynamic DNA methylation and demethylation processes seems crucial to mammalian development and pathogenesis, we strove to understand the impact of

epigenetic modifications on mutagenesis by exploring the roles of 5hmC and 5caC in modulating UV-induced DNA damage.

Skin (Cells) as an Attractive System

The skin provides an attractive system for studying normal cellular processes as well as cancer pathogenesis, since skin cells are abundant and easily accessible. Normal human skin is covered by a stratified epidermis that functions as a self-perpetuating barrier against harmful microbes, dehydration and other insults (Fuchs, 2008). This protection is maintained by a tightly regulated balance of cellular proliferation, differentiation and apoptosis within the skin cells (Gniadecki *et al.*, 1997; Chaturvedi *et al.*, 1999; Fuchs, 2008).

The epidermis forms the top protective covering of normal skin, and is itself composed of multiple layers from the stratum corneum or horny layer at the top to proliferating cells in the basal layer that are anchored to the basement membrane. Keratinocytes constitute the majority of the epidermis, with some melanocytes to protect the deeper skin layers from harmful UV rays. The bottom layer of epidermal keratinocytes contains a single layer of basal, proliferative keratinocytes that give rise to daughter cells and progressively move outward and commit to terminally differentiate as they expand (Alonso and Fuchs, 2003; Fuchs, 2008). As differentiating keratinocytes move upwards into the spinous layer and then granular layer, and finally into the horny stratum corneum and exit at the skin surface (Alonso and Fuchs, 2003)—a process that takes approximately one month in human epidermis—their network of 10-nm keratin intermediate filaments strengthens to form IF cables that distribute force over an entire tissue by anchoring to desmosome junctions (Alonso and Fuchs, 2003). Once they have reached

the surface after major morphological changes, the differentiated keratinocytes have now become "enucleated cellular skeletons" that are continually sloughed at the surface and replaced by inner cells moving outward in a dynamic flux (Fuchs, 2008).

The decreased incidence of skin cancers seen in individuals with darker skin may be attributed both to protective UV filtering and a more efficient removal of UV-damaged cells (Miyamura *et al.*, 2007; Yamaguchi *et al.*, 2006; Liu and Fisher, 2010). As a first line of defense, melanin pigments prevent UV-induced DNA damage upon sun exposure. Melanin is synthesized by melanocytes in the epidermis, and then distributed by neighboring keratinocytes into the upper skin layers. In addition to skin, melanin can also be found in hair, retina, iris and parts of the central nervous system (Yamaguchi and Hearing, 2009).

Given their attractiveness as a model system and their direct relevance to studying UV damage, human and mouse skins, as well as the various primary cells (keratinocytes, melanocytes, fibroblasts) derived from them, have been popularly used as a supplement to immortalized cancer cell lines. Throughout the multiple projects I pursued during my graduate years, primary human keratinocytes and melanocytes were extensively used in conjunction with other systems to better mimic biological processes. In fact, observations in primary skin cultures often formed the basis for generating new hypotheses.

Purpose and Hypothesis

Originally, we were looking into a question related to, but slightly different from the focus of this thesis—whether UV irradiation has any effect on the methylation and demethylation of cytosine. Initial pilot immunofluorescence experiments suggested that in primary human skin cells (dark

as well as white primary melanocytes, primary keratinocytes, and primary fibroblasts), 5hmC expression was significantly enhanced within 3 hours of UV irradiation; we were encouraged by a lack of similar observation in cancer cells, since TET enzymes are mutated or downregulated in multiple cancers. Although loss-of-function mutations in TET genes have not been found in human solid tumors yet, mutations in TET genes were frequently found in hematological malignancies, and downregulation of TET expression was observed in human breast, liver, lung, pancreatic and prostate cancers (Wu and Ling, 2014). This correlates with reduced 5hmC levels in various tumors, as 5hmC reduction can result from loss-of-function mutations in TET genes and from inhibition of TET activity through reduced α-ketoglutarate (oxoglutarate) levels or increased 2-hydroxyglutarate levels (via IDH1/2 mutations) (Yang *et al.*, 2013). Among the currently known mutations in TET genes, the MLL-TET1 (t(10;11)(q22;q23) translocation was identified in acute myeloid leukemia and acute lymphoblastic leukemia, while a deletion of 2p23 was seen in myelodysplastic syndrome, and a range of nonsense/missense/frameshift mutations and deletions was found in the cysteine-rich region or catalytic domain of TET2 (Kinney and Pradhan, 2013). My preliminary analysis of TET mutations in skin cutaneous melanoma (Broad, Cell 2012; The Cancer Genome Atlas; Yale, Nature Genetics 2012; cBioPortal for Cancer Genomics) revealed a large number of C to T or CC to TT missense transition mutations in TET1/2/3 (see Chapter 3 for further discussion). However, the lack of reliable DNA demethylation antibodies at the time (back in 2010), in addition to technical concerns about false positives from UV crosslinking, led us to hand over this project to multiple collaborators (whose recent mass spectrometry results seem to validate our original observations).

Therefore, in moving forward, we modified our objectives: For this thesis, we are building upon current understanding of the effect of cytosine methylation on photoproduct

formation and mutagenesis, and extending our studies into the rapidly evolving field of hydroxymethylation and carboxylation. We hypothesize that 5-hydroxymethylcytosine and 5-carboxylcytosine are part of a protective, TET-mediated DNA demethylation pathway for 5-methylcytosine, and thus they will mitigate UV-induced photoproduct formation, in contrast to enhanced CPD formation by the 5-methyl moiety.

CHAPTER TWO

TETrify against UV: 5hmC and 5caC protect from UV-induction of CPDs

Intrastand CPD dimers and their well-known UVB-signature mutations have been linked to basal cell carcinoma and squamous cell carcinoma (Brash *et al.*, 1991), and there is a strong association between melanoma risk and UVB exposure (Fears *et al.*, 2002). The most prevalent UVB-induced DNA lesion, CPDs are both abundant and mutagenic, and their repair is slow and inefficient. CPDs are premutagenic lesions for cytosine to thymine transitions, the UVB signature mutations (LeClerc *et al.*, 1991; Otoshi *et al.*, 2000). In human basal and squamous cell carcinomas, these mutations have been found especially in trinucleotide sequences containing 5-methylcytosine (Tornaletti and Pfeifer, 1995; You and Pfeifer, 2001; Lee and Pfeifer, 2003; Cannistraro and Taylor, 2009). The C to T transition process at dipyrimidine sequences involves deamination of cytosine, and methylation at the C-5 carbon of cytosine both enhances dimerization and promotes deamination, leading to enhanced CPD formation and increased UVB signature mutations (Douki and Cadet, 1994; Tommasi *et al.*, 1997; You *et al.*, 1999; Douki *et al.*, 2000; Mitchell, 2000; Cannistraro and Taylor, 2009; Rochette *et al.*, 2009). The TET machinery can oxidize 5meC into 5hmC and 5caC (Gong and Zhu, 2011; Shen *et al.*, 2013; Song *et al.*, 2013; Song and He, 2013). 5hmC levels are reduced in melanomas, oral squamous cell carncioma, brain tumors and other cancers (Lian *et al.*, 2012; Gambichler *et al.*, 2013; Jäwert *et al.*, 2013), correlating with TET mutations or downregulation in multiple cancers (Wu and Ling, 2014). Since 5hmC and 5caC are part of a TET-mediated DNA demethylation pathway, and methylation has been associated with enhanced formation of premutagenic UVB lesions, we studied the effects of hydroxylation and carboxylation on UVB induction of CPD dimers.

Methodology

Our approach to studying the effect of epigenetics on UV-induced CPD formation was to first choose an *in vitro* system to validate previous findings on 5meC (Douki and Cadet, 1994; Tommasi *et al.*, 1997; You *et al.*, 1999; Douki *et al.*, 2000; Mitchell, 2000; Cannistraro and Taylor, 2009; Rochette *et al.*, 2009). While DNA dot blots previously worked well for quantifying levels of 5meC and 5hmC, they could not be used for measuring CPD formation, as UVC crosslinking (which was requisite to bind samples to the dot blot membrane) distorted subsequent measurements of UVB-induced CPDs.

Therefore, we optimized an ELISA assay from Cosmo Bio, Inc., for our *in vitro* tests on modified oligonucleotides. Compared to standard sandwich ELISAs, our protocol incorporates an additional biotin-conjugated antibody in order to enhance signal intensity. We first tested out our protocol on genomic (herring sperm and calf thymus) DNA as well as 18bp-oligonucleotides, both under single-stranded (heated) and double-stranded (non-heat-denatured) conditions, before proceeding to assay optimization with the desired 11bp-modified oligonucleotides (single-stranded). Under optimized conditions [1:1000 anti-cylobutane pyrimidine dimers monoclonal antibody (Cosmo Bio USA), followed by 1:2000 biotin-xx $F(ab')_2$ fragment of goat anti-mouse IgG (Life Technologies) and 1:5000 peroxidase-streptavidin in order to enhance signal intensity detected at 490 nm with 8 mg/20mL O-phenylenediamine dihydrochloride (Sigma Aldrich) (stopped by 2M H_2SO_4)], we could show that 5meC enhances UV-induced CPD dimer formation, in agreement with previous literature as described above.

Since a flanking guanine base has been shown to enhance CPD formation and accelerate cytosine deamination through the oxidation potential of its O6 group (Cannistraro and Taylor, 2009), we firstly chose a set of oligonucleotide sequences flanked by guanine, reasoning that differential responses to UVB-induced photodimer formation will be more distinguishable if we used a master sequence that promotes maximal induction. Our initial set of modified oligonucleotides comprises the following sequences: 5'-AAAAAAAACXG-3' and 5'-AAAAAAAATXG-3', where X= C, 5meC, 5hmC, 5caC, T. For experiments with double-stranded DNA, we designed oligonucleotides with a CpG dinucleotide in the middle (in order to avoid artificial outlier observations that might have resulted from a terminal cytosine): 5'-ATATXGATATA-3'/5'-TATATXGATAT-3', X=C, 5meC, 5hmC.

In proceeding with experiments with genomic DNA extracted from TET overexpressing A2058 melanoma cells (either overexpressing full-length active TET2 (FL2) or mutant TET2 (mut)) from the lab of our collaborator, Professor Yujiang Shi at BWH (Lian *et al.*, 2012), we found that simply adapting our assays for cellular DNA does not always work. Cells were grown to confluencies ranging from 50-70%, irradiated with a UVB lamp at various doses, and harvested in lysis buffer at set time points. Genomic DNA was extracted by a phenol/chloroform protocol (during my rotation project, I had assessed the relationship between UV dose, cell confluency, and sensitivity to apoptosis in primary melanocytes and keratinocytes—while some of the cells we used to study the effects of epigenetic modifications on UV photoproducts are not primary, my earlier work revealed the optimal range of UV doses and DNA extraction protocols (coated spin columns versus gravity columns versus phenol/chloroform organic separations) to use in cells). We suspected that *in vitro* assays may respond to DNA of different lengths with bias, and so I first sonicated genomic samples (Bioruptor sonicator; Diagenode) for a range of

sonication durations, ran them on 2.5% agarose gels to check for even smear patterns, and selectively tested out in ELISA assays. The ELISA assays I had previously optimized for oligonucleotides worked best with briefly sonicated (5 min or 10 min) DNA that was heat-denatured; however, this assay only worked with certain antibodies against photoproducts from a Japanese company (Cosmo Bio), but did not work with 5meC or 5hmC antibodies (even though those results were beautiful and extremely sensitive for our 11 bp oligos). Thus, I proceeded to test out other antibodies, as well as a 5hmC ELISA kit (Zymo Research Corporation) that was previously published (in testing unsonicated, genomic DNA across range of tissues); as it turns out, that kit did not work either, even their own controls barely fit on a standard curve, raising doubts about the accuracy of commercially available 5hmC kits.

In order to compare and contrast the levels of 5hmC, 5meC and 5caC between cells with different TET expressions, I went back to dot blots. As explained above, the membrane crosslinking required for sensitive detection undermined quantification of photo-dimers, but does not hinder detection of epigenetic markers such as 5hmC. The dot blots had a preference for sonicated DNA (any sonication time seemed to work well), and heat denaturation did not seem to be necessary (unlike ELISA assays). Also, I found that for the 5meC (EMD Biosciences) and 5hmC (ActiveMotif) antibodies selected, the dot blots worked better, and more consistently, on Hybond-N+ nylon (GE Healthcare Life Sciences) membranes instead of nitrocellulose membranes (which a previous collaborator, A. Rao, had advised for their own 5hmC antibody).

For broadspectrum UVB irradiations, we used two Stratagene UVB light bulbs at doses ranging from 100 mJ/cm^2 to 4 J/cm^2 (based on insights from previous unrelated side-projects on oligonucleotides, primary and cancer cell lines, skin explants, and mice). For UVA irradiations, we used two Stratagene blacklight bulbs at doses ranging from 1 J/cm^2 to 40 J/cm^2. UVB/UVA

emittance was measured with an ILT1400 photometer (International Light Technologies, Inc.) equipped with a UVB-1 SEL240 probe or UVA SEL033 probe, respectively. For UVC irradiations, we used two 15 W 254 nm germicidal bulbs (Stratagene) at timed doses (2-20 min). UVC doses were measured with a Thorlabs power meter (with a 250 nm filter) by recording and manually integrating a Watts versus time plot.

Controls and Addressing Potential Pitfalls

In addition to testing commercial standards (Cell Biolabs, Inc.; Zymo Research Corporation) to validate our ELISA assays, we also designed our own positive and negative controls (custom modified oligonucleotides from Eurofins MWG Operon served as epigenetic standards; various cellular DNA verified by immunofluorescent staining, as well as calf thymus DNA under known conditions, served as standards for photoproducts). Since our oligonucleotides of interest were all 11 bp long, we used a representative sequence (oligo #6 = 5'-AAAAAAAATCG-3') to establish a standard curve (Figure 1). This revealed an optimal DNA concentration of 0.1188 μM (20 ng/50μl for oligo #6), which showed a fairly linear CPD dimer vs. UV dose response curve (Figure 2). We used these DNA concentrations throughout our ELISA assays on oligonucleotides and cellular DNA to ensure consistency (except in cases of high absorbance values, where we performed dilutions as necessary). Additional tests using mouse IgG (the Cosmo Bio antibodies against CPDs, 6-4 PPs and Dewar isomers were all monoclonal, mouse) were performed to test the quality of the antibodies. ELISA experiments using mouse IgG or with any missing subsequent antibodies did not show any UV induced increase in absorbance values, as expected.

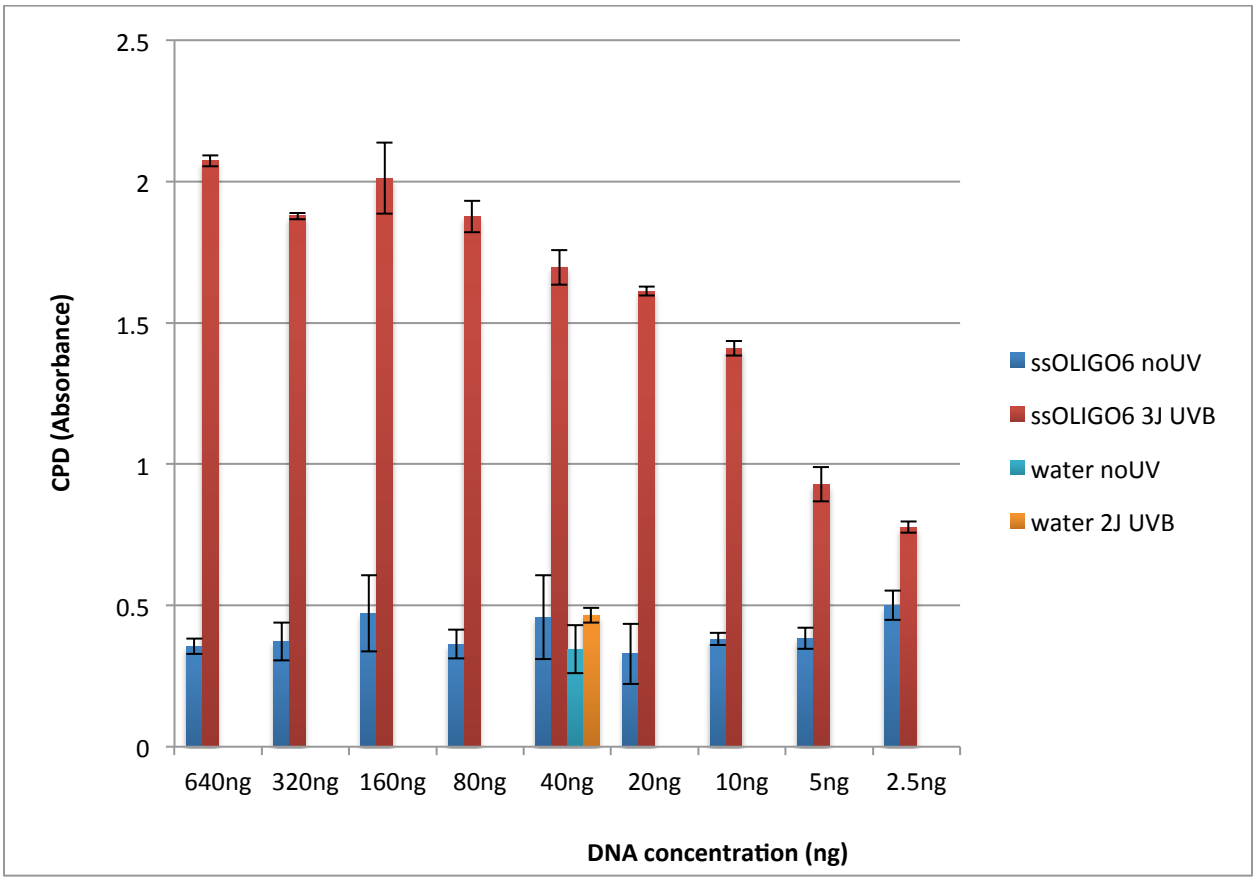

Figure 1: Standard curve for CPD detection by ELISA (n= 3).

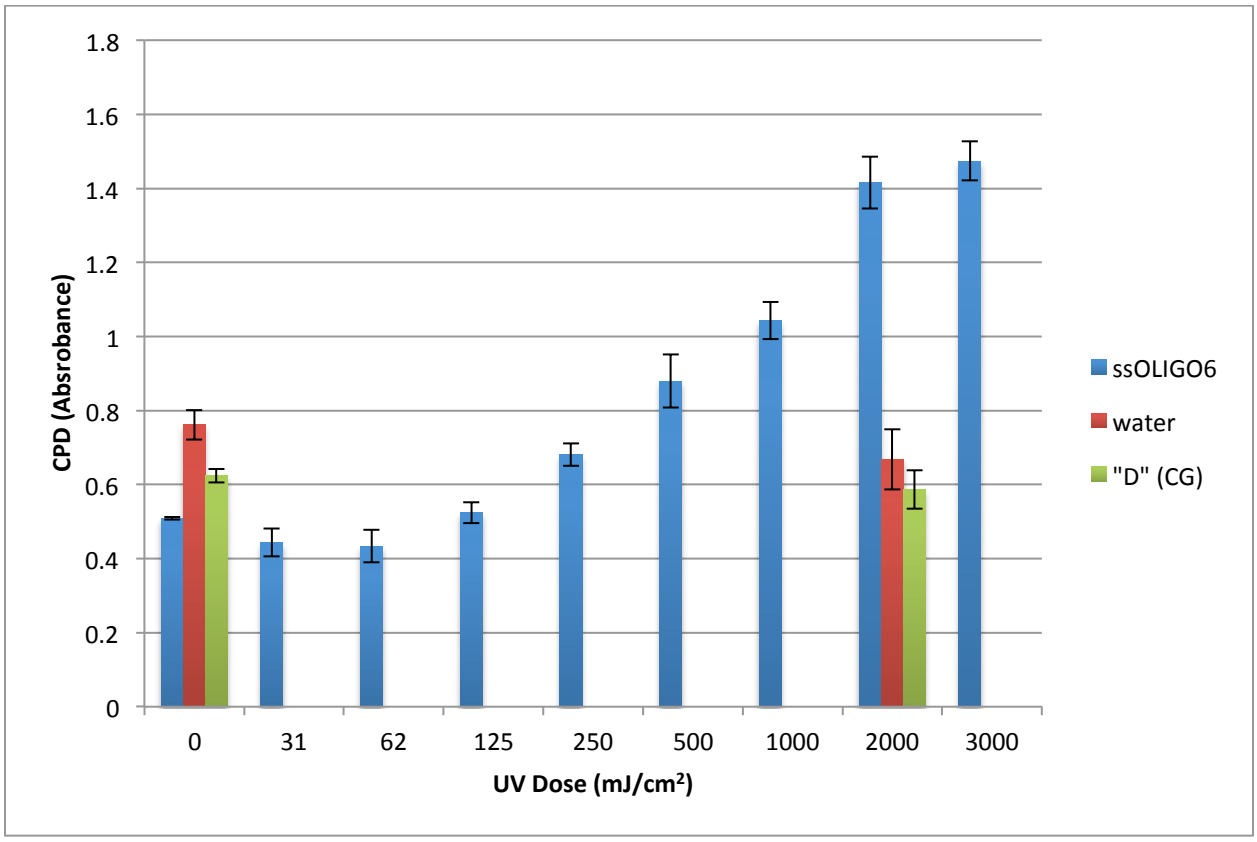

Figure 2: ssOligo6: CPD induction vs UVB dose (ELISA, n= 3).

We had several other concerns about using ELISA assays to measure the levels of photoproduct inductions. In case any reductions in CPD levels detected for 5hmC oligonucleotides were not due to the hydroxymethyl moiety but to instability upon irradiation, we decided to test the stability of the hydroxymethyl moiety. Our results do not suggest any hydroxymethyl instability upon broadspectrum UVB irradiation (Figure 3a). Similarly, the 5meC moiety did not display any instability upon UV irradiation (Figure 3b). Figure 3 (and other data, not included here) also shows that our oligonucleotides contain the correct modified bases as specified.

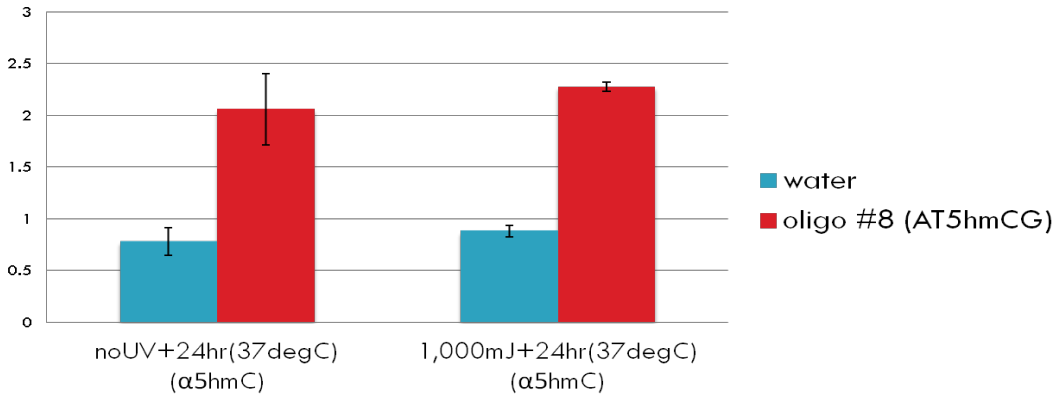

Figure 3a: 5hmC stability in oligonucleotides unaffected by UV irradiation/time/heat (ELISA, y-axis: 5hmC (absorbance), n= 3).

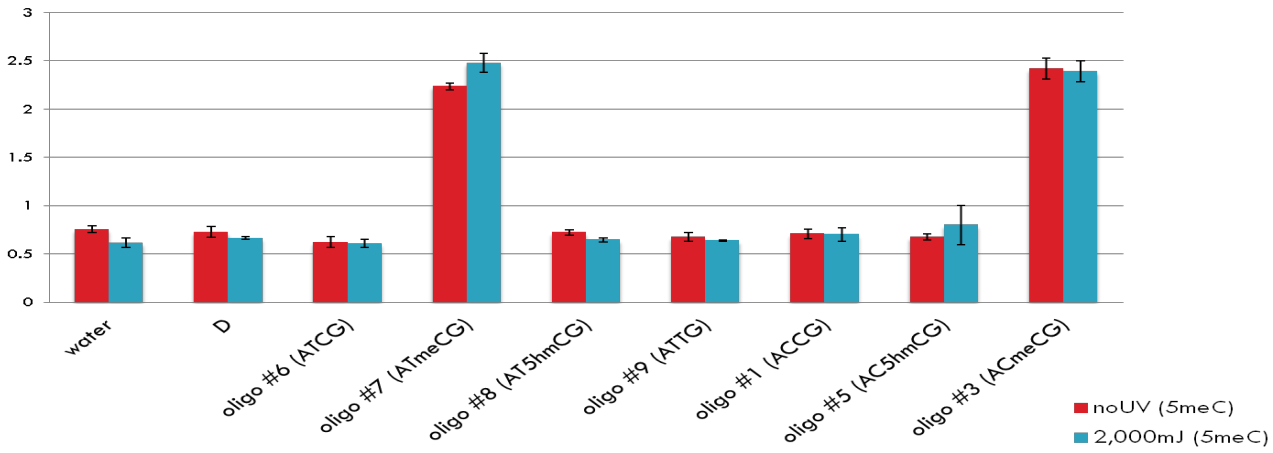

Figure 3b: 5meC stability in oligonucleotides unaffected by UVB treatment (ELISA, y-axis: 5meC (absorbance), n= 3).

As another measure of quality control, we tested the levels of CPD dimers in our single-stranded oligonucleotides both immediately after UV-treatment and after 24 hr (in a warm room, 37ºC). For oligonucleotides that were significantly photodimerized with 1 J/cm^2 broadspectrum UVB, we saw a 30-40% reduction in CPDs after 24 hr exposure to heat and light (Figure 4). This does not conflict with current knowledge that the dimerization of CPDs is reversible (Witkin, 1975; Szekeres *et al.*, 1976).

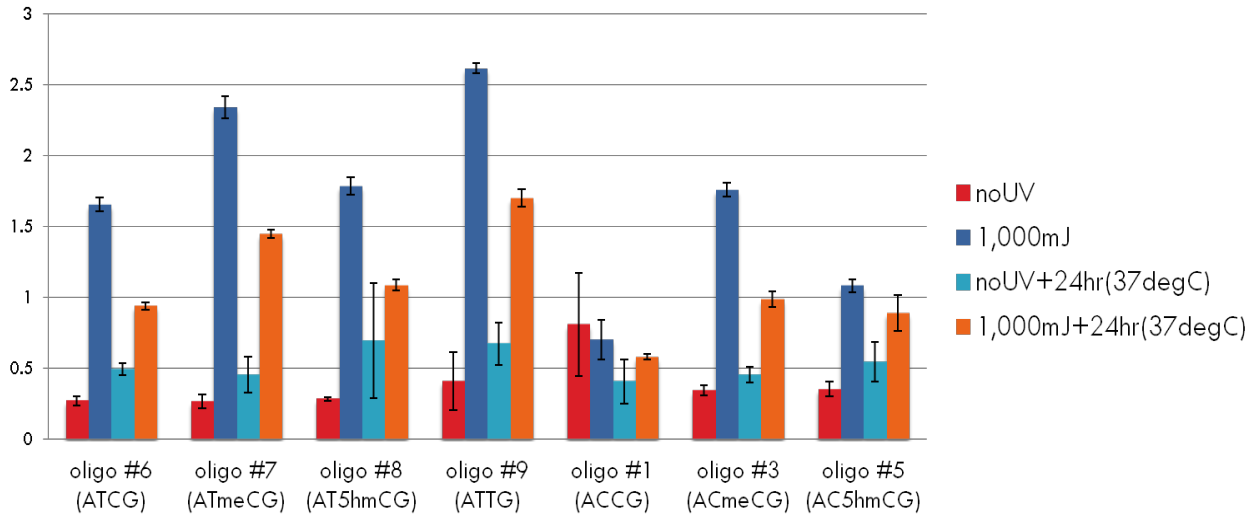

Figure 4: Reduction of UV-induced CPD dimers with time
(ELISA, y-axis: CPD (absorbance), n= 3).

Furthermore, we were concerned about the high background absorbance measured at both 490nm and 450nm, despite diluting antibody concentrations. Since many instruments fail to follow the Beer-Lambert law (for linearity) at absorbance units above 2 (corresponding to light transmittance below 1%), it was important to bring down the background in order to obtain more meaningful signal: noise ratios. I found it necessary to individually optimize assay conditions for different sample groups (e.g., more dilute DNA concentrations for sequences containing a thymine) in order to be able to obtain meaningful (and comparable) observations. Switching from an HRP-based reading to a luminescence output did not improve our ELISA assays. However, we found that prolonging the blocking step cut down background signals in half, and reduced the variability in our samples as well (Figure 5).

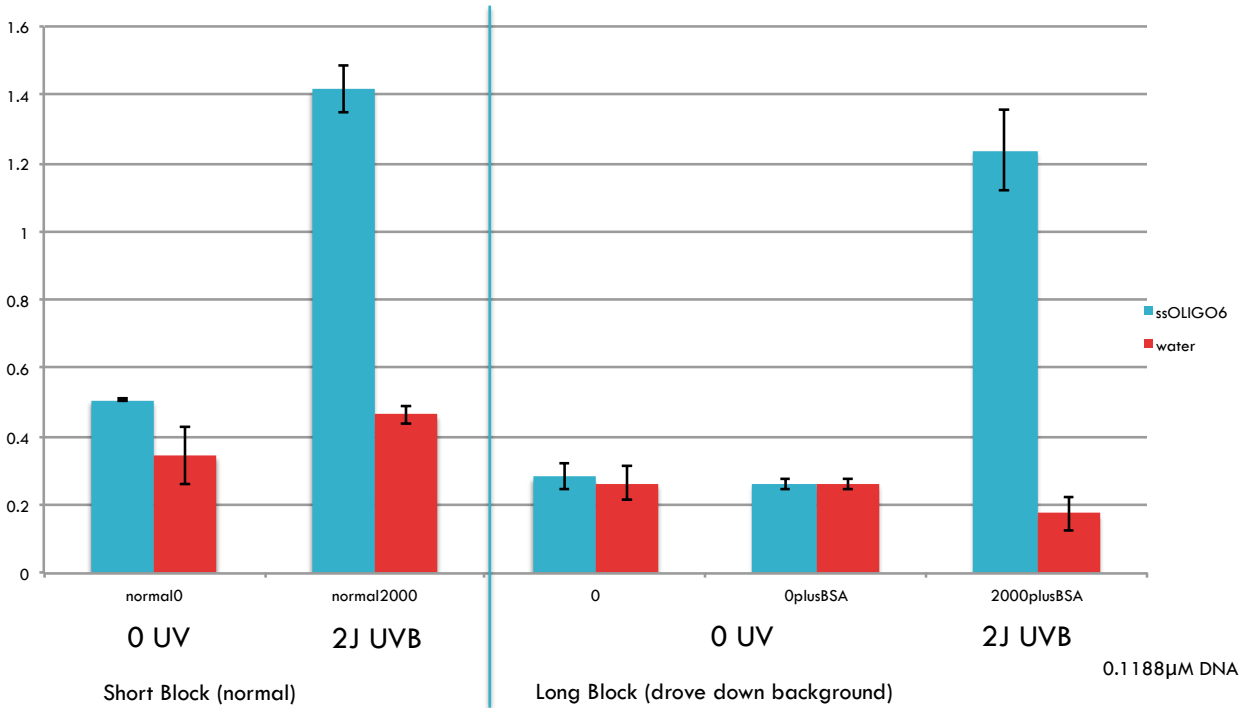

Figure 5: Impact of block duration on signal detection (ELISA, y-axis: CPD (absorbance), n= 3).

Results

Our first aim was to test the hypothesis that a methyl moiety at the C-5 position enhances UV induction of CPD dimers. In ELISA tests with our first set of single-stranded oligonucleotides (detailed above), we observed trends consistent with those published in recent literature (Douki and Cadet, 1994; Tommasi *et al.*, 1997; You *et al.*, 1999; Douki *et al.*, 2000; Mitchell, 2000; Cannistraro and Taylor, 2009; Rochette *et al.*, 2009). More specifically, we observed up to 4-fold enhanced CPD induction (red versus orange bars, Figure 6) in the presence of a methylated cytosine (with 10-fold signal:noise ratios).

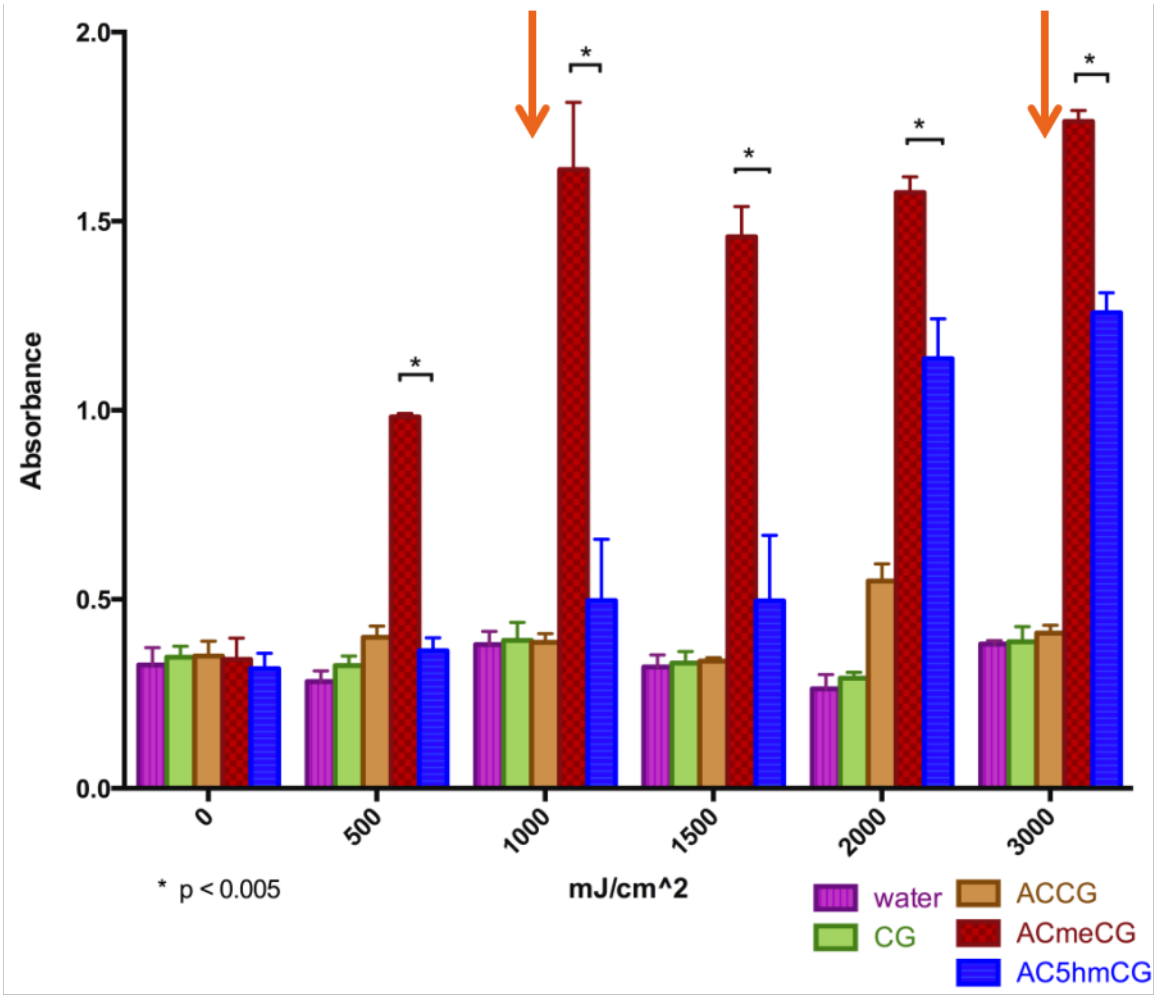

Figure 6: CPD induction by UVB in ACXG oligonucleotides
(ELISA, y-axis: CPD (absorbance), n≥ 3, unpaired t tests).

Our second aim was to establish whether a hydroxymethyl moiety would reduce or even protect from UV-induced CPD dimer formation. Since hydroxylation of 5meC by TETs initiates demethylation, we hypothesized that the hydroxymethyl moiety would have effects opposite to enhanced inductions seen with a 5-methyl moiety. As predicted, our results indicated that the 5-hydroyxmethyl moiety on cytosine mitigates methylation-related CPD enhancement upon UV irradiation. Depending on sequence context, UV-induced formation of CPDs was up to 3-fold lower for 5hmC-containing oligonucleotides than their 5meC counterparts (Figure 7). 5hmC's

protective effect on the UV response was also upheld in duplex oligonucleotides, although at a lower ratio but still with statistical significance (Figure 8).

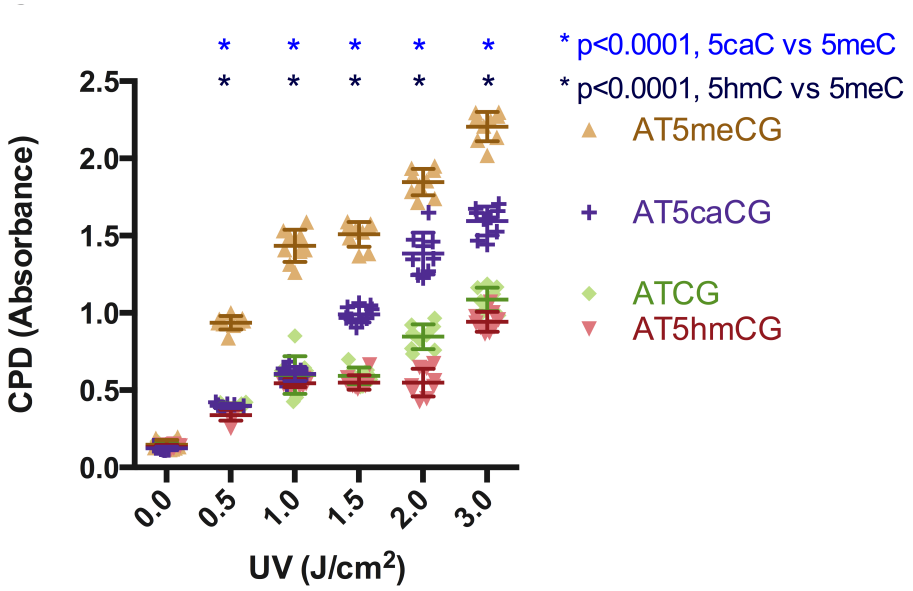

Figure 7a: Shielding from UV-induced formation of ATXG CPDs (ELISA, n= 9, multiple unpaired t tests).

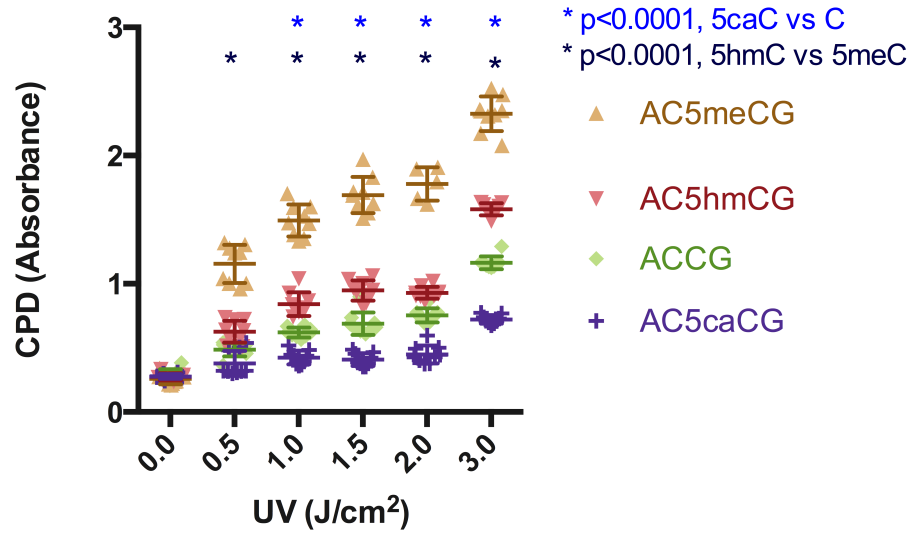

Figure 7b: Shielding from UV-induced formation of ACXG CPDs (ELISA, n≥ 5, multiple unpaired t tests).

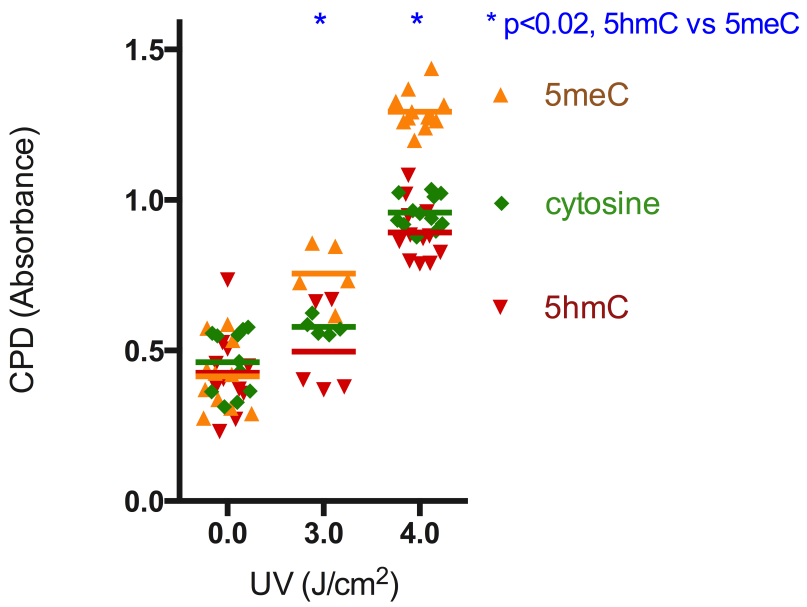

Figure 8: UV induction of CPDs in duplex ATXGAT
(ELISA, n≥ 5, unpaired t test).

As we were validating our results in a cellular model, we decided to repeat and extend our studies to include 5-carboxylcytosine (initially omitted from oligo designs), another TET-oxidized product of 5meC (downstream of 5hmC). As a DNA demethylation intermediate, we hypothesized that 5caC would also mitigate UV induction of CPDs. Similar to 5hmC, our results showed that CPD formation was up to 3-fold lower for 5caC-containing oligonucleotides than their 5meC counterparts (Figure 7). This protective effect was especially pronounced in the AC5caCG sequence context.

Part of our interest in 5caC was sparked by the technical advances made by our collaborator, Prof. Y. Yang at UC Riverside, which enabled the quantification of TET-oxidized products of 5meC, including 5hmC and 5caC (Liu *et al.*, 2013). Yet another reason was the recent publication of a paper on the formation of CPDs in 5hmC-containing dipyrimidines (Kim

et al., 2013). Their work on 5hmC CPD dimers validated some of our *in vitro* data, as their oligonucleotides shared sequence similarities with ours (we designed our study to detect maximum differences), and they used similar high UV doses similar as well. However, by postulating a protective role for 5hmC and 5caC in the UV induction of photoproducts, we sought to expand our work beyond an *in vitro* proof-of-existence story for 5hmC-containing CPD dimers. Technical limitations (difficulty of designing 5fC-containing oligonucleotides) led us to postpone extending our studies to 5-formylcytosine (5fC) as well, another novel DNA demethylation intermediate (between 5hmC and 5caC).

As a third aim, we set out to validate our observations in a more biologically relevant system with a cell model from our epigenetics collaborator, Prof. Y. Shi at BWH. We used Prof. Shi's previously established melanoma cell model that contains abundant 5meC but negligible 5hmC levels (Lian *et al.*, 2012). By DNA dotblot with antibodies against 5hmC and 5meC (Figure 9a), we saw that overexpression with a full-length active TET2 led to increased 5hmC levels. 5hmC measurements by ImageJ software from the NIH after background adjustments (automatic light background with rolling ball radius of 50.0 pixels) were as follows: At 1 µg DNA dilution, 29281.894 area for TET2+ versus 8485.430 area for TET2- cells (3.34:1), at 800 ng DNA dilution, 30802.723 versus 6882.752 (4.48:1), at 400 ng DNA dilution, 34423.614 versus 5856.095 (5.88:1), at 200 ng DNA dilution, 35924.555 versus 22472.782 (1.60:1); hence, at a non-saturated dilution of 400ng DNA, there was a maximum 5.88:1 or 1:0.17 5hmC ratio for TET2+:TET2- cells. 5meC measurements by ImageJ software from the NIH after background adjustments (automatic light background with rolling ball radius of 50.0 pixels) were as follows: at 1 µg DNA dilution, 7893.255 area for TET2+ versus 10949.255 area for TET2- cells (1:1.39); at 800 ng DNA dilution, 9057.497 versus 12467.376 (1:1.38); at 400 ng DNA dilution, 7670.255

versus 11471.255 (1:1.50); at 200 ng DNA dilution, 5899.134 versus 10936.134 (1:1.85); at 100 ng DNA dilution, 7062.477 versus 10315.770 (1:1.46); at 50ng DNA dilution, 10047.134 versus 10195.205 (1: 1.01). Given the strong saturation of 5meC dots at multiple DNA dilutions (indicating abundance of 5meC in cellular DNA) for both TET2+ and TET2- cells, as well as the arbitrary surface area estimations by ImageJ, the best estimate of 5meC ratios for these cells was an average of ratios from all serial dilutions, which was 1:1.43 or 0.70:1 for TET2+:TET2- cells.

Previous studies have shown that both UV irradiation of intact cells and naked DNA produced similar distributions of CPD inductions, although the cellular environment decreased the apparent UV dose by 50% through shielding of the nuclear DNA (Lippke *et al.*, 1981). Furthermore, recent mass spectrometry data has shown that natural 5hmC levels only reach a fraction of 5meC cellular levels (<15% in human brain, <10% in mouse brain, <20% in HEK cells, <5% in mouse skin (Liu *et al.*, 2013)). Given the overshadowing abundance of 5meC relative to 5hmC in our cellular model, as well as the reduction in apparent UV dose through cellular shielding, the protective effect in TET2-overexpressing cells was statistically significant only at the highest UV dose. At 3J/cm^2 of UVB (Figure 9b), induction of cyclobutane pyrimidine dimers was significantly lower ($p<0.0003$) in TET2 overexpressing cells (with higher levels of 5hmC) than in TET2 mutant cells. These results are in agreement with the protective effect we observed in our oligonucleotide studies noted earlier. Taken together with novel evidence for loss of 5hmC as an epigenetic hallmark of melanoma (Lian *et al.*, 2012; Gambichler *et al.*, 2013), our results suggest that 5hmC offers protection from UV-induced cyclobutane pyrimidine dimer formation, and thus TET oxidation of 5meC might be a cellular mechanism to protect against UV damage.

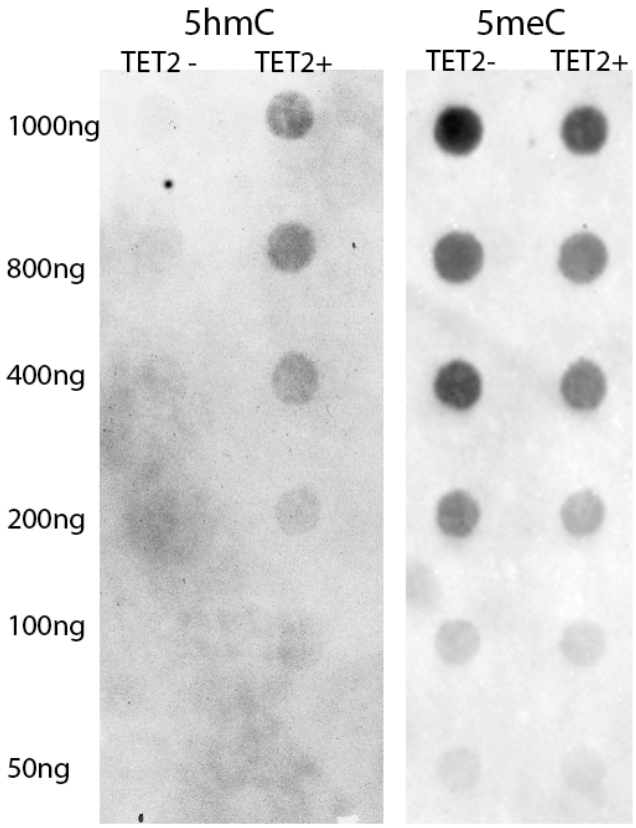

Figure 9a: 5hmC and 5meC levels in melanoma cells (DNA dotblot, serial dilutions).

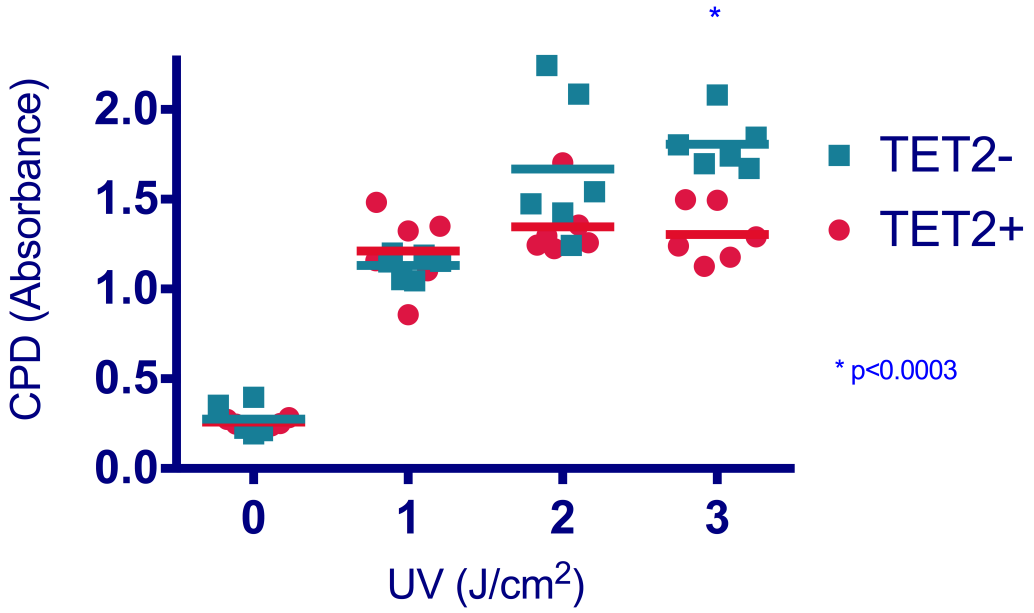

Figure 9b: CPD induction by UV in melanoma cells (ELISA, n≥ 5, unpaired t test).

From *in vitro* studies of UV irradiated plasmid DNA, we could assume 0.3 CPDs per 10^8 daltons of DNA per 1 J/m^2 of UVB irradiation, or 2.4 CPDs per 10^8 daltons of DNA per 1 J/m^2 of UVC irradiation (Mitchell *et al.*, 1991). Using simple math assumptions (~650 dalton/bp), and the highest dose of UV that I used for both cells and oligo experiments (3J/cm^2 for UVB, 3.2 J/m^2 for UVC)--this comes to 58,500 CPD/million bp under UVB or 499,200 CPD/million bp under UVC. From the previous discussion of induction ratios (see Chapter 1), the ratio of TT: CT + TC: CC CPDs after UVB irradiation range from 40:40:20 to 52:40:7 (Mitchell *et al.*, 1991). Therefore, of the 58,500 CPD/million bp, about 40% or 23,400 CPD/million bp would contain a cytosine. This would translate into 70.2 million cytosine-containing CPDs across a human genome with 3 billion base pairs.

We saw that UV-induced formation of CPDs was up to 3-fold lower (70% reduction) for 5hmC-containing oligonucleotides than their 5meC counterparts (Figure 7). With about 3% of all cytosines methylated in human DNA, and a maximum of 5% of all 5meC hydroxylated in skin (Liu *et al.*, 2013), even a 70% shielding would only lead to a 3.5% overall protection for a rare 5hmC subpopulation. This could translate into 2.5 million fewer CPDs per cell (3.5% of 70.2M) under the UVB doses that I used. The protective shielding by 5hmC against UVB-induced CPDs is probably most influential through context dependence: Just as we observed a sequence dependence for the extent of 5hmC's shielding (Figures 7, 8), it is plausible that 5hmC may have a bigger impact in certain regulatory and tumor suppressor genes. For example, a large proportion of invasive SCCs contain UVB signature mutations in the p53 gene (Brash *et al.*, 1991), and over a third of these p53 mutations contain 5meC trinucleotides (Tornaletti and Pfeifer, 1995; You and Pfeifer, 2001; Lee and Pfeifer, 2003; Cannistraro and Taylor, 2009), even

though only a small fraction of all cytosines is methylated across the human genome. Since the loss of 5hmC has been associated with numerous cancers, including melanoma (Lian *et al.*, 2012; Gambichler *et al.*, 2013), perhaps the protective effect from a rare 5hmC in a cell is enhanced through sequence context and its location in a pivotal gene like p53. Furthermore, it has been previously shown that the frequency of CPD formation oscillates along the DNA backbone, with maximum induction near sites farthest from the surface of core histones, and minimum induction near sites closest to the surface of core histones (Gale *et al.*, 1987). If the genome were preferentially hydroxylated at sites farthest away from histone surfaces, the protective effect from a rare yet potent 5hmC could significantly reduce the formation of premutagenic CPD lesions.

Contributions: Prof. Geno Y. Shi (Brigham/Women's Hospital, Harvard) provided frozen vials of both TET2+ and TET2- cells, while I performed all sample preparations and biochemical assays (ELISAs, dot blots, UV treatments).

CHAPTER THREE

To protect or not to protect: 5hmC's dual roles in modulating photoproduct formation

In addition to CPDs, another type of intrastrand DNA lesion is (6-4) photoproducts (6-4 PPs). Depending on the chemical nature of the two pyrimidine bases involved and other parameters, both the yield and the ratio between CPDs and 6-4 PPs upon UV irradiation can vary greatly (Douki, 2006). Like CPDs, 6-4 PPs are premutagenic lesions for cytosine to thymine transitions; however, 6-4 PPs are also premutagenic lesions for thymine to cytosine transitions (LeClerc *et al.*, 1991; Otoshi *et al.*, 2000). We extended our *in vitro* studies into 6-4 PPs by using the same ELISA and dotblot assays as above; therefore, the methodology and controls were similar to those in Chapter 2.

Results

Further experiments investigating how DNA demethylation intermediates modulate UV formation of photoproducts have revealed an interesting duality for 5-hmC. Both single-stranded (Figure 10a) and double-stranded (Figure 10b) 5hmC-containing oligonucleotides, as well as genomic DNA extracted from UV-irradiated TET2-overexpressing cells, showed statistically significantly enhanced UV induction of (6-4) photoproducts (Figure 10c). In oligonucleotides, methylation at the C-5 position did not alter UV induction of 6-4 PPs, while carboxylation at the C-5 carbon hindered 6-4 PP formation, which is in line with our hypothesis and earlier results showing 5caC's protective shielding from UV induction of CPDs.

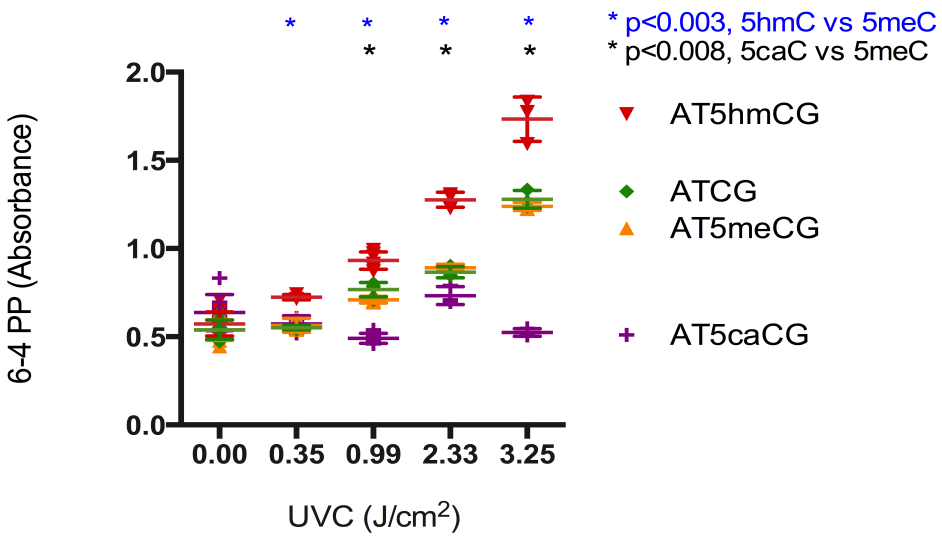

Figure 10a: 5hmC enhances UVC-induced formation of 6-4 PPs (ELISA, n≥ 3, multiple unpaired t tests).

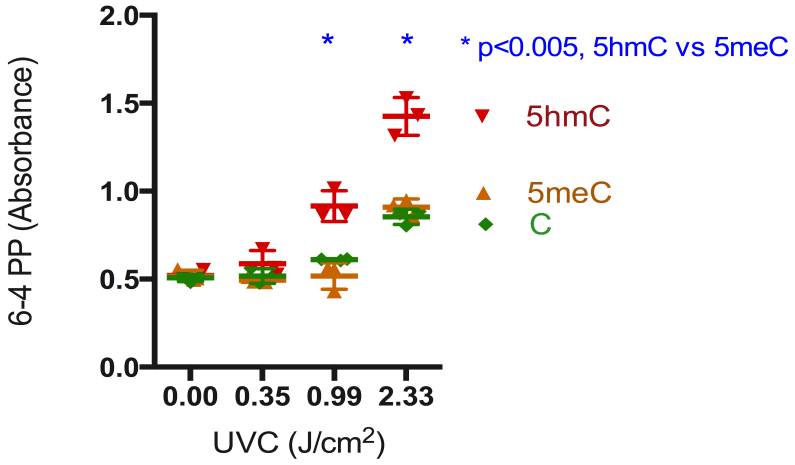

Figure 10b: UV induction of 6-4 PPs in duplex ATXGAT (ELISA, n= 3, unpaired t test).

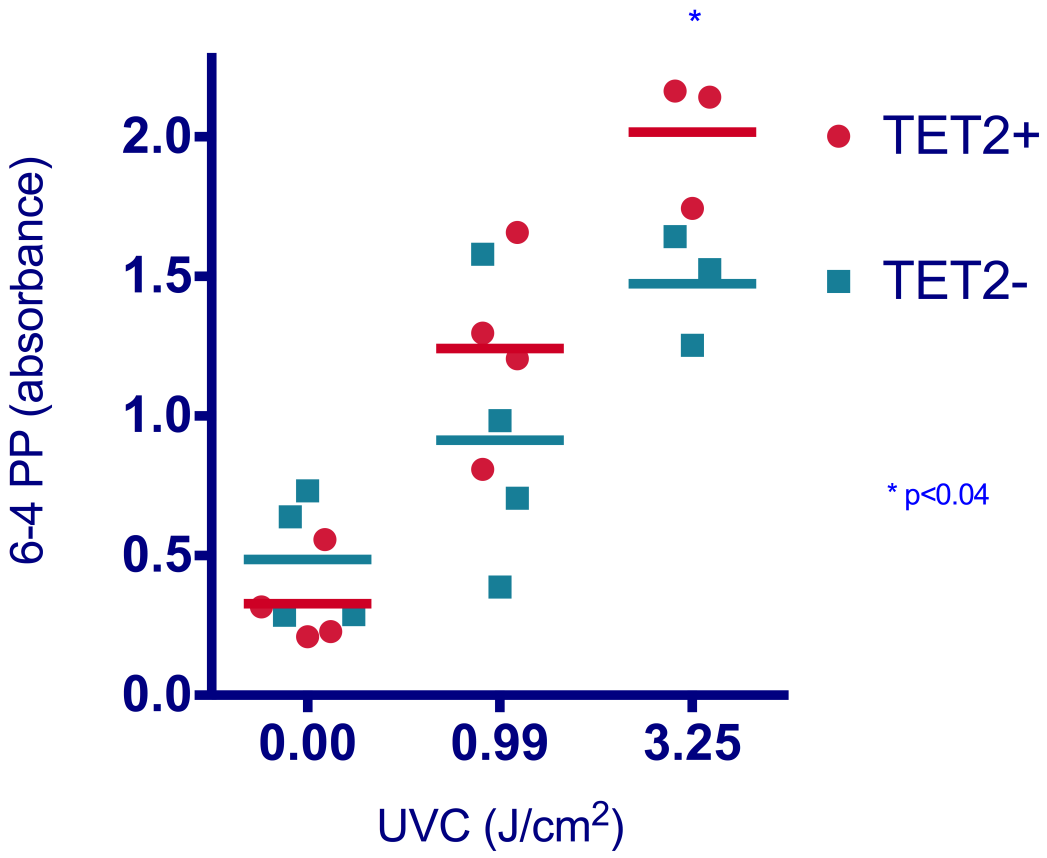

Figure 10c (Continued): 6-4 PP induction by UVC in melanoma cells (ELISA, n≥ 3, unpaired t test).

Contrary to our expectations, the presence of 5hmC increased UV inductions of 6-4 PPs by 30% or more (Figure 10). UVC (Figure 10a) was a more potent inducer of 6-4 PPs than (broadspectrum) UVB (Figure 11a), while UVA failed to induce any detectable levels of 6-4 PPs. In cells, TET2 overexpression failed to enhance 6-4 PP formation under UVB (Figure 11c), but did with statistical significance under a high UVC dose (Figure 10c). Furthermore, hydroxylation-mediated 6-4 PP enhancement was pronounced for ATXG sequences (Figure 11a), but absent for ACXG sequences (Figure 11b). This is consistent with current knowledge

that 6-4 PPs are formed at 5'-TC-3', 5'-CC-3', and 5'-TT-3', but not at 5'-CT-3' sites in DNA (Häder and Sinha, 2005).

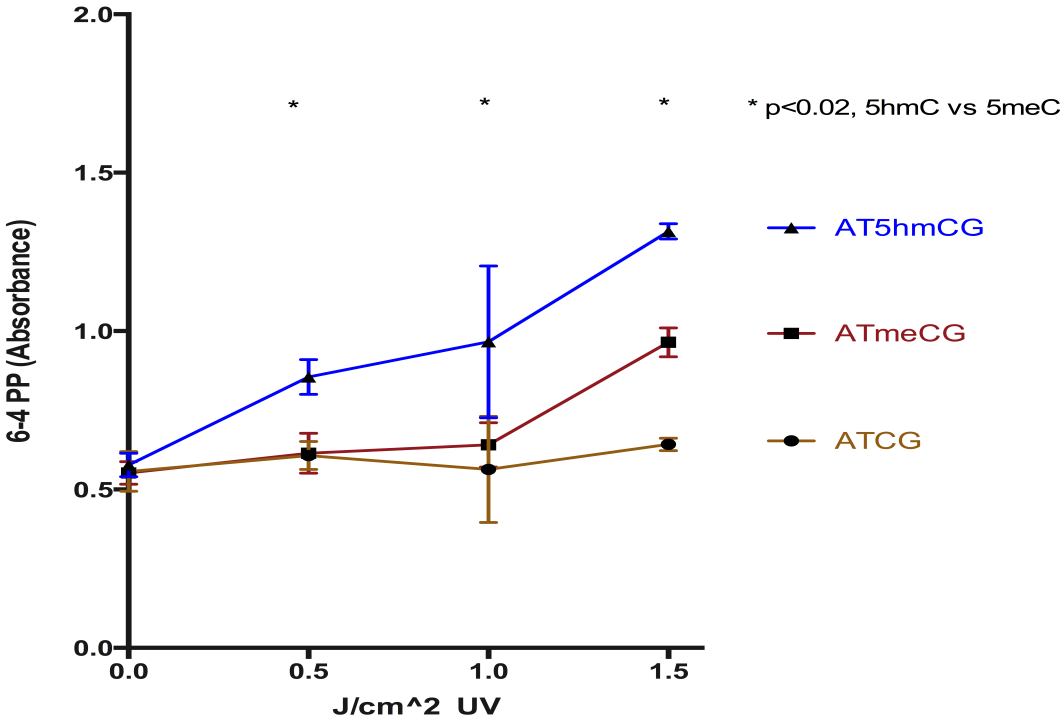

Figure 11a: 6-4 PP induction by UVB in ATXG oligonucleotides (ELISA, n≥ 3, unpaired t test).

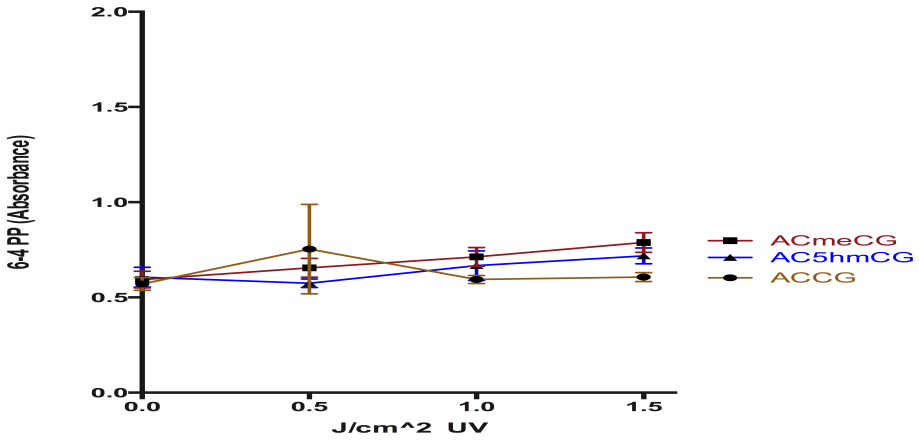

Figure 11b: 6-4 PP induction by UVB in ACXG oligonucleotides (ELISA, n≥ 3, unpaired t test: p>0.05).

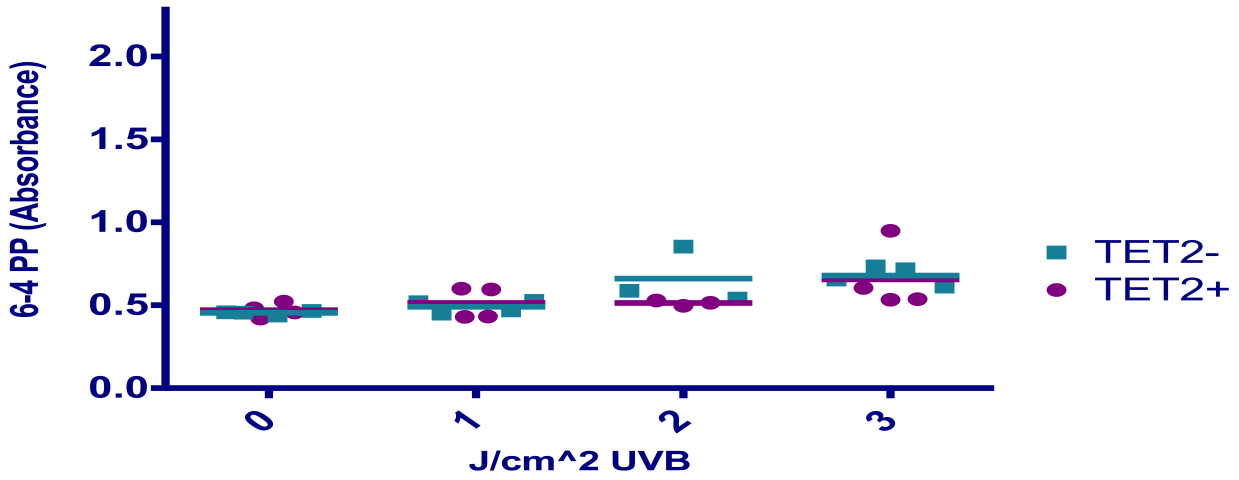

Figure 11c (Continued): 6-4 PP induction by UVB in melanoma cells
(ELISA, n≥ 3, unpaired t test: p>0.05).

For additional validation of 5hmC's apparent enhancement of 6-4 PPs, we irradiated TET1/2 double-knockout (DKO) embryonic stem cells (from Y. Shi's lab, Brigham/ Women's Hospital, Harvard). Wild type (WT) embryonic stem cells had high levels of 5hmC, while TET1/2 DKO embryonic stem cells had low levels of 5hmC, as expected (Figure 12a). By DNA dotblot with antibodies against 5hmC, 5hmC measurements by ImageJ software from the NIH after background adjustments (automatic light background with rolling ball radius of 50.0 pixels) were as follows: At 1 µg DNA dilution, 74123.597 area for WT versus 1170.991 area for DKO cells (63.3:1), at 800 ng DNA dilution, 69681.342 versus 1471.527 (47.4:1), at 400 ng DNA dilution, 60932.907 versus 210.192 (289.9:1), at 200 ng DNA dilution, 52798.333 versus 3011.962 (17.5:1); at 100 ng DNA dilution, 49106.312 versus 5848.421 (8.4:1); hence, at a non-saturated dilution of 200ng DNA, there was a maximum 17.5:1 or 1:0.06 5hmC ratio for TET1/2 WT:DKO cells. After UVC irradiation, the 5hmC-containing WT embryonic stem cells

enhanced induction of 6-4 PPs (p-value < 0.0001), in contrast to 5hmC-depleted TET1/2 DKO embryonic stem cells (Figure 12b). These results agreed with earlier results from melanoma cells, where TET2 overexpression (and correspondingly high 5hmC levels) led to enhanced UVC induction of 6-4 PPs (Figure 10c). While low-5hmC TET2- melanoma cells showed moderate UVC induction of 6-4 PPs (Figure 10c), UVC irradiation of low-5hmC TET1/2 DKO embryonic stem cells did not lead to significant 6-4 PP formation. This difference could potentially be explained by the significantly lower 5hmC ratio in the embryonic stem cells (1:0.06 for TET1/2 WT:DKO) than in the melanoma cells (1:0.17 5hmC ratio for TET2+:TET2-), if 5hmC functions to enhance UV induction of 6-4 PPs. Therefore, our loss-of-function experiments with TET1/2 DKO embryonic stem cells complemented our gain-of-function experiments with TET2 overexpressing melanoma cells.

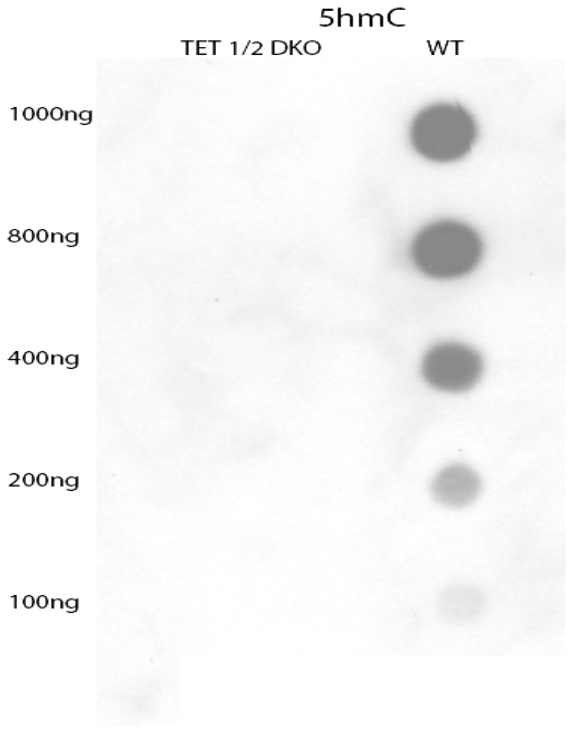

Figure 12a: 5hmC levels in embryonic stem cells (DNA dotblot, serial dilutions).

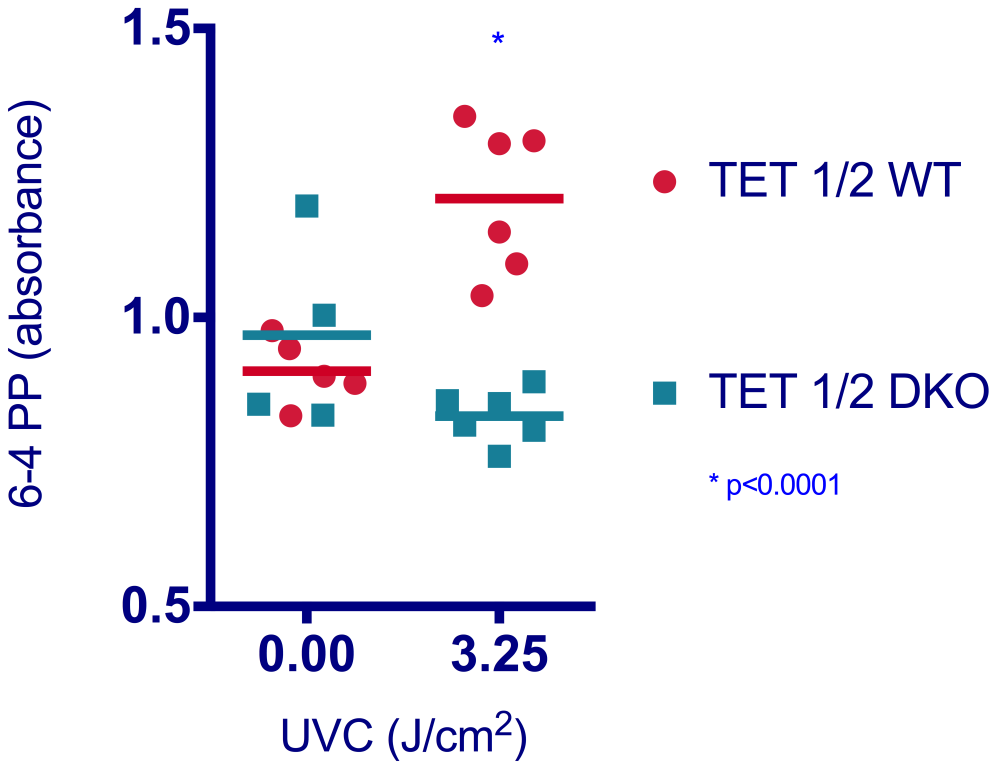

Figure 12b (Continued): 6-4 PP induction by UV in TET1/2 DKO embryonic stem cells (ELISA, n≥ 4, unpaired t test).

To explain the discrepancy between our hypothesis and 5hmC's apparent dual effects on UV induction of photoproducts, we turned to structural modeling. Structures were generated visualized using UCSF Chimera (Pettersen *et al.*, 2004). We used the structure of a T-T photoproduct from the Protein Data Bank (PDB ID: 1CFL) (Lee *et al.*, 1999). Assuming similar structural distortions in DNA for T-T and T-C 6-4 photoproducts (Kim and Choi, 1995), we converted the structure to a T-C photoproduct in an ATCG context using the *swapna* and *Build Structure* commands. We followed the structural description given by Douki (Douki, 2006). Modifications on the 5-position of the cytosine were incorporated using the *Build Structure*

command, and structures were then minimized using the *Minimize Structure* command. Following this, the *Find Clashes/Contacts* command was used to find pseudobonds.

Structural modeling and Chimera visualization identified an additional potential hydrogen bond for the T-5hmC (6-4) photoproduct (Figure 13), suggesting a lower energy transition state for 5hmC. Just as 5meC promotes the dimerization reaction with an adjacent 3'-cytosine (see discussion above in Chapter 1, introduction), leading to enhanced UV induction of CPD formation, a more favored transition state for the T-5hmC (6-4) photoproduct could explain 5hmC's duality in modulating the UV response. In addition to a lower energy transition state, the hydroxyl group may stabilize a T-5hmC radical, or promote DNA bending that would be favorable to forming a (6-4) adduct, as NMR spectroscopy data and structural calculations (Kim and Choi, 1995) suggested a 44 degrees distortion in the overall DNA helix. Yet a more bulky carboxyl group may counter any favorable energy stabilization and prevent (6-4) photoproduct formation through steric hindrance. Future structural studies such as free energy calculations are needed to further elucidate the rationale behind 5caC-containing oligonucleotides' shielding effects (other than the absence of a dimerization-promoting 5-methyl group). The correlation between the presence of the hydroxymethyl moiety and (6-4) photoproduct formation is consistent with our model (see Chapter 4) of 5hmC as a selective epigenetic shield against UV damage, diminishing cyclobutane pyrimidine dimer formation while enhancing UV induction of (6-4) photoproducts.

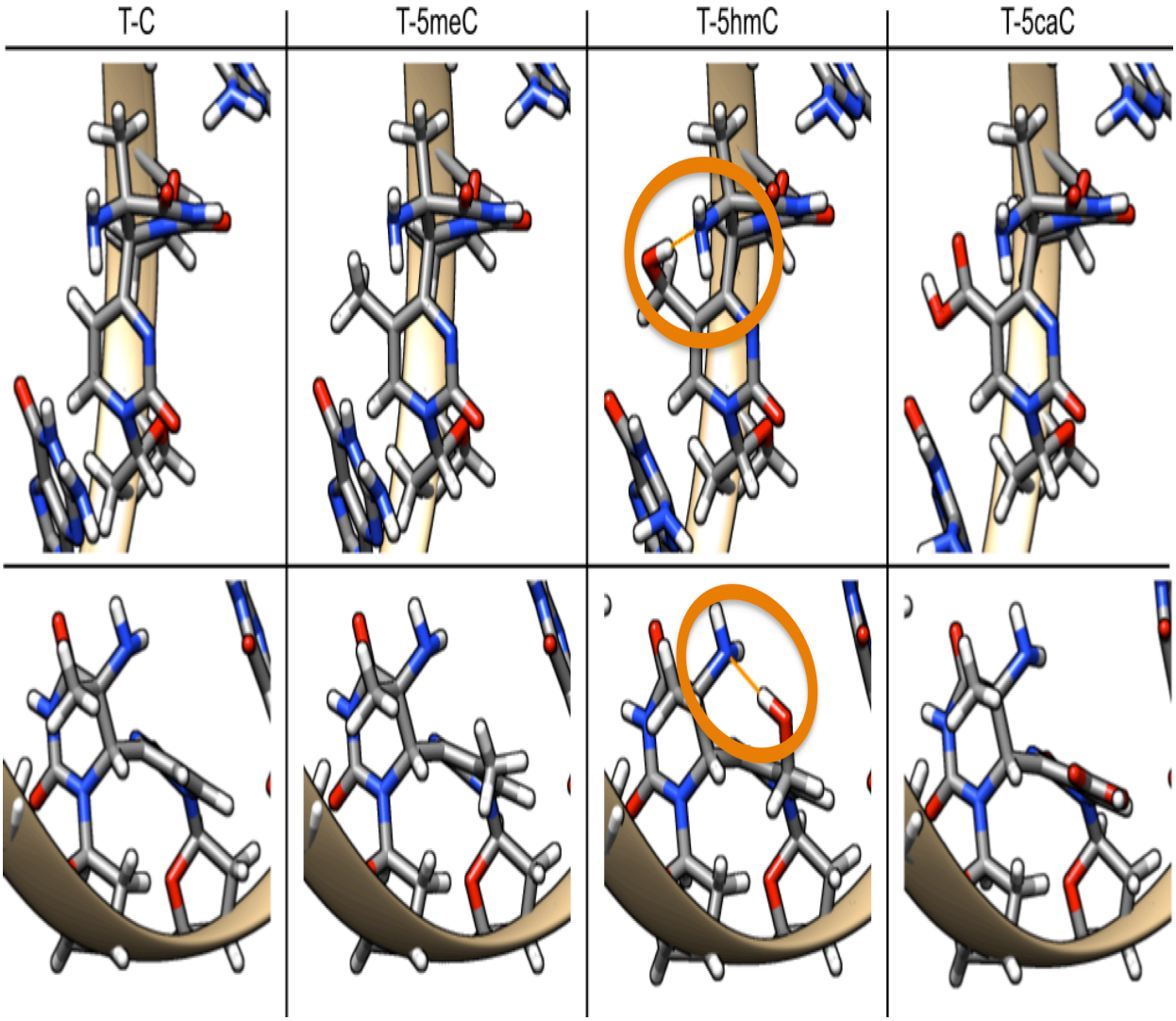

Figure 13: Structural models of T-C photoproducts (with M. Stefan, HMS)
Upper panel: Front view, lower panel: side view.
The pseudobond identified by Chimera for T-5hmC is shown in orange.

We found no significant induction of Dewar isomers in any of our oligonucleotides or genomic DNA under UVA or UVB irradiation (Figure 14). Dewar isomers are much more unstable than 6-4 PPs (Kan *et al.*, 1992). Current literature suggests Dewar isomers of 6-4PPs mainly to be a UVC event and a two-step process. First, in synthetic processes, short oligomers (usually containing a thymine-thymine sequence) are irradiated under UVC (254nm), whereupon

TT 6-4 PPs are purified by HPLC. Next, these purified intermediates are irradiated under 320nm (UVA) to produce Dewar valence isomers (Yamamoto *et al.*, 2006).

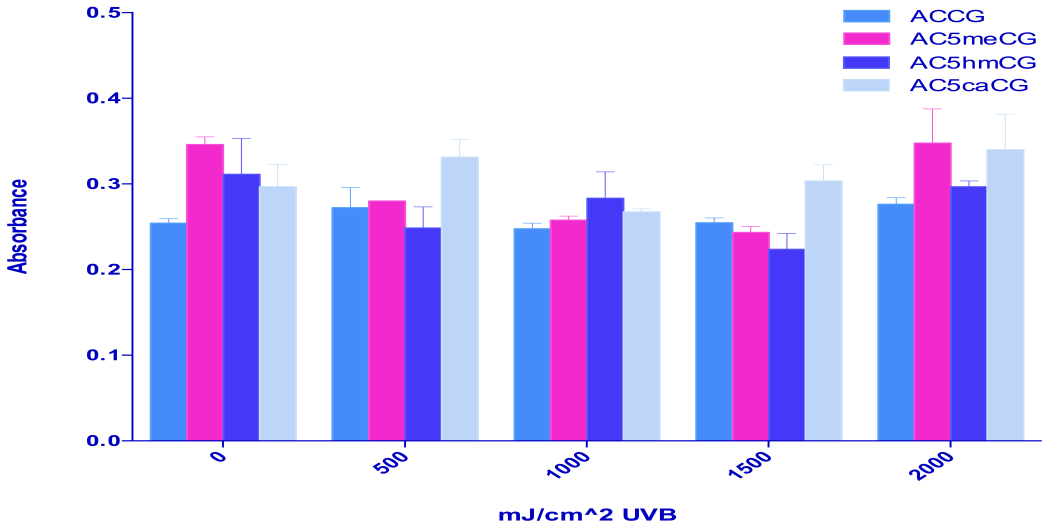

Figure 14: Comparison of Dewar valence isomers after UVB irradiation (ELISA, y-axis: Dewar (absorbance), n≥ 4).

Contributions: Prof. Geno Y. Shi (Brigham/Women's Hospital, Harvard) and his postdoctoral fellow, Christian Argueta, provided TET2+/ TET2- melanoma and TET1/2 DKO ES cell. I performed all sample preparations and biochemical assays (ELISAs, dot blots, UV treatments), as well as bioinformatical analyses. Structural modeling using Chimera (UCSF) was done together with Melanie Stefan (Harvard Medical School). Mass spectrometry was done by S. Liu and Prof. Y. Wang (UC Riverside).

CHAPTER FOUR: DISCUSSION

Highlights

- 5hmC and 5caC protect from UV-induced formation of cyclobutane pyrimidine dimers
- 5hmC also enhances UV-induced formation of (6-4) photoproducts
- 5hmC's duality upon UV damage is coupled to TET2 (over)expression

We have shown that 5meC enhances UV induction of CPDs in accordance with published literature (Douki and Cadet, 1994; Tommasi *et al.*, 1997; You *et al.*, 1999; Douki *et al.*, 2000; Mitchell, 2000; Cannistraro and Taylor, 2009; Rochette *et al.*, 2009). Furthermore, in a new model (Figure 15), we have shown via both modified oligonucleotides and melanoma cells that hydroxylation and carboxylation of 5meC by TET2 shield from CPD dimer induction. In addition, we point out a completely novel, contradictory role for 5hmC—enhancement of UV-induced (6-4) photoproduct formation, potentially through a more favorable T-5hmC 6-4 PP transition state.

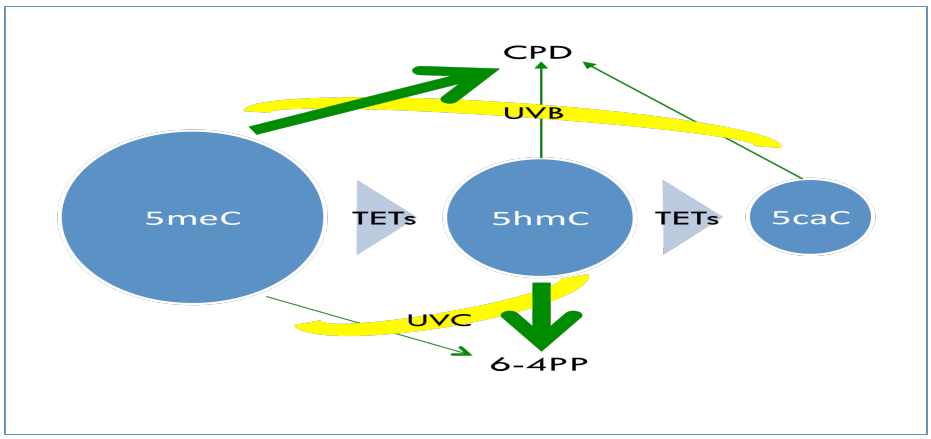

Figure 15: Model.

We started with *in vitro* experiments measuring UV induction of photoproducts in various modified oligonucleotides. Given that a flanking guanine base enhances CPD formation and accelerates cytosine deamination (Cannistraro and Taylor, 2009), we firstly focused on a set of oligonucleotide sequences flanked by guanine, reasoning that differential responses to UV-induced photodimer formation will be more distinguishable if we used a master sequence that promotes maximal induction. We optimized a biotin-enhanced ELISA assay in which 5-methylation of a single cytosine in the oligonucleotides enhanced UV-induced CPD formation for both ATXG and ACXG sequences, in accordance with previously published *in vitro* studies. Our ELISA results also indicated that both the 5-hydroxymethyl and 5-carboxl moieties diminish methylation-enhanced CPD formation upon UV irradiation. Since both 5hmC and 5caC are TET-mediated DNA demethylation intermediates, it is not surprising that they would have the opposite effect of the methyl moiety by reducing methylation-related CPD enhancement.

Our observation of diminished UV induction of CPDs in DNA demethylation intermediates was also upheld in duplex oligonucleotides, as well as melanoma cells. We used a TET2 overexpression cell model designed by our collaborator Prof. Y. Shi. In addition, new experiments (by Y. Shi's lab) with TET1/2 double-knockout embryonic stem cells (low 5hmC levels) showed a 2-4 fold increase in CPDs by immunofluorescent staining when compared to wild-type embryonic stem cells. While these loss-of-function results are still preliminary, they complement our gain-of-function results with TET2 overexpressing cells. Since the loss of 5-hydroxymethylcytosine and inactivation of the TET enzymes have been implicated in skin cancers, and repeated exposure to UV radiation is a known risk factor for developing skin cancers, our data suggest a link between DNA demethylation and UV damage.

Further experiments on UV induction of Dewar isomers and 6-4 PPs revealed a lack of significant Dewar isomer formation under UVA/UVB, but significantly enhanced UVB/UVC induction of T-5hmC 6-4PPs. We attributed this to the different mutagenic properties of (6-4) photoproducts (capable of both C to T and T to C transition mutations). Structural modeling and Chimera visualization revealed an extra hydrogen bond between an amine group of thymine and a hydroxyl group on the adjacent cytosine, indicating a lower transition state for T-5hmC 6-4 PPs. Our data suggest that upon UV damage, 5hmC may drive DNA lesion formation toward (6-4) photoproducts, leading to diminished CPD induction and enhanced 6-4 PP induction.

Depending on the chemical nature of the two pyrimidine bases involved, the wavelength of the incident photons, the stability of the duplex DNA, the ionic strength, and other parameters, the yield and the ratio between CPDs and 6-4 PPs inductions can vary greatly (Douki, 2006). Furthermore, the frequency of photoproduct formation oscillates along the DNA backbone with an average periodicity that is similar to the average repeat for the DNA helix (Gale *et al.*, 1987). Since photoproduct formation requires local bending of the DNA helix, the frequency of photoproduct formation is reduced at sites closest to the surface of core histones, as histone binding to DNA would physically restrain movement in the DNA backbone (Gale *et al.*, 1987). Compared to CPDs, this oscillatory dependence should be more limiting for the induction of 6-4 PPs, which require a more severe distortion of up to 44 degrees in the DNA (Kim and Choi, 1995). If there is a similar distribution pattern for hydroxylation/ demethylation along the DNA helix, the modulatory effects of a rare 5hmC on UV-induced photoproduct formations would be quite significant. In fact, while the presence of premutagenic photoproducts is required for mutations, mutation hot spots in human cells are determined by DNA structural features instead of photoproduct frequencies (Brash *et al.*, 1987).

In shuttle vector mutation studies, UVB irradiation produced more mutations (insertions/deletions/transition mutations) than UVC irradiation; this also correlated with increased formation of cytosine containing CPDs under UVB (Keyse *et al.*, 1988). While both CPDs and 6-4 PPs are premutagenic lesions for cytosine to thymine transition mutations, CPDs are responsible for the majority of UVB signature mutations in mammalian cells (Brash *et al.*, 1987; LeClerc *et al.*, 1991; Otoshi *et al.*, 2000). In fact, in repair-deficient xeroderma pigmentosum group A cells, CPDs were responsible for generating 90% of transition mutations (Brash *et al.*, 1987). Additionally, 6-4 PPs are excised at double the rate of excision for CPDs in human, hamster and mouse cells (Mitchell *et al.*, 1985; Mitchell *et al.*, 1992). This more efficient removal of 6-4 PPs is also a very fast process, as over 70% of 6-4 PPs are removed within 4-6 hr after irradiation, compared to 17 hr for CPDs (Mitchell *et al.*, 1985). 6-4 PPs' lower mutagenic potential and faster removal make them less toxic to cells than CPD lesions. Therefore, our observations that 5hmC drives UV induction of photoproducts toward 6-4 PPs and away from the more mutagenic CPDs is in alignment with our model of UV damage protection through hydroxylation and DNA demethylation.

As new interest develops in the (rediscovered) DNA demethylation intermediates, evidence emerges for their diverse regulatory functions, ranging from developmental reprogramming to recruiting chromatin-altering binding proteins (Shen *et al.*, 2013; Song *et al.*, 2013; Song and He, 2013). Our findings assign a new function to 5hmC and 5caC—as selective epigenetic shields against UV damage, contributing to the dynamic network of DNA methylation and demethylation that regulates mammalian pathogenesis.

Future Pursuits

More thorough studies can be carried out through a comprehensive set of sequence variations (flanking base, placement of moiety, length of oligonucleotide). In addition, we can complement (and validate) our TET overexpression gain-of-function data with TET- and DNMT-knockout loss-of-function cell models.

Another goal we can pursue is to link CPD formation to methylation sites via a modified co-IP-ELISA on genomic DNA. This is a technically challenging feat, but the principle is straightforward: Since we are postulating that hydroxylation protects cytosines from methylation-enhanced, UVB-induced damage, we expect to see more CPD dimers formed at 5meC than 5hmC post-UVB. We are planning to essentially separate 5meC and 5hmC populations from irradiated, TET2+ genomic DNA (by co-IP, both sequences will be tested and reversed as control), and then assaying for CPD levels by our ELISA protocol. An alternative might have been ChIPSeq, except that the bioinformatics world does not seem to think current 5hmC or 5meC antibodies reliable enough for ChIPSequencing (based on discussions with Prof. Jun Song at UCSF), but we will not be attempting to reinvent any technical wheels. We could build on previous knowledge acquired during my year-long training with our previous mass spec collaborator (R. Giese, on interstrand adducts project, see Appendix), where a sequence of dual digestions with NP1 and PDE was used to cleave genomic DNA down to single nucleotides (as verified on HPLC). From here on, we will proceed with co-IP assisted by agarose beads, and ultimately followed by CPD ELISA as optimized before. A similar experiment could be performed to link 6-4 PP formation to hydroxymethyl sites on genomic DNA.

Yet another question we can address is whether modulation of photoproduct formation by 5hmC and 5caC lead to reduced/ increased mutations. CPD-mediated C to T transition (especially in the p53 tumor suppressor gene) is the UV signature mutation for non-melanoma skin cancers. We expect that an analysis of the p53 mutation spectra (from the International Agency for Research on Cancer TP53 Database) to reveal the majority of UV mutations within methylated cytosine sequences. We expect that the correlation between mutation frequency and sequence specificity to agree with the trends we observe from our oligonucleotide studies.

Furthermore, our collaborator Prof. Y. Shi has shown that loss of 5hmC is an epigenetic hallmark of melanoma, as well as an indicator for melanoma progression (Lian *et al.*, 2012). Injection of TET-depleted stem cells into mice led to aggressive and proliferative tumorigenesis, while injection of wild-type stem cells into mice only led to differentiated benign teratomas (Koh *et al.*, 2011; Münzel *et al.*, 2011). A preliminary analysis of TET mutations in TCGA skin cutaneous melanoma (cBioPortal for Cancer Genomics) revealed that C to T or CC to TT transitions accounted for a majority of their TET1/2/3 mutations (Figure 16), including one highly mutagenic nonsense mutation in TET1 (Figure 16a).

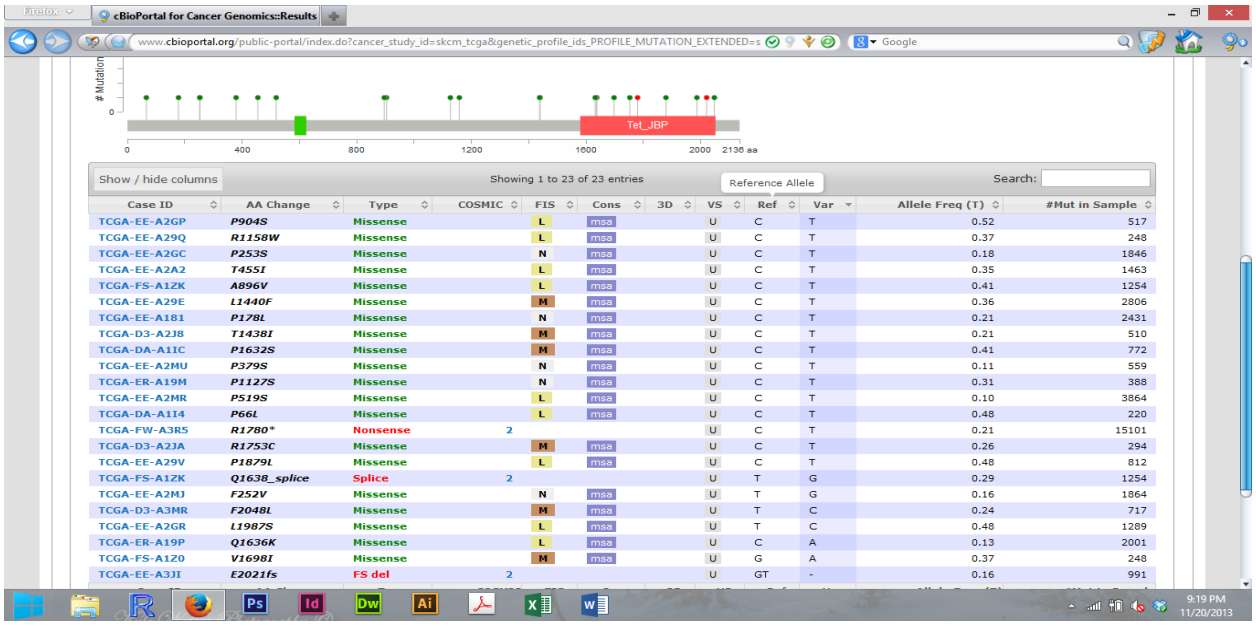

Figure 16a: TET1 mutations in skin cutaneous melanoma (TCGA, cBioPortal for Cancer Genomics).

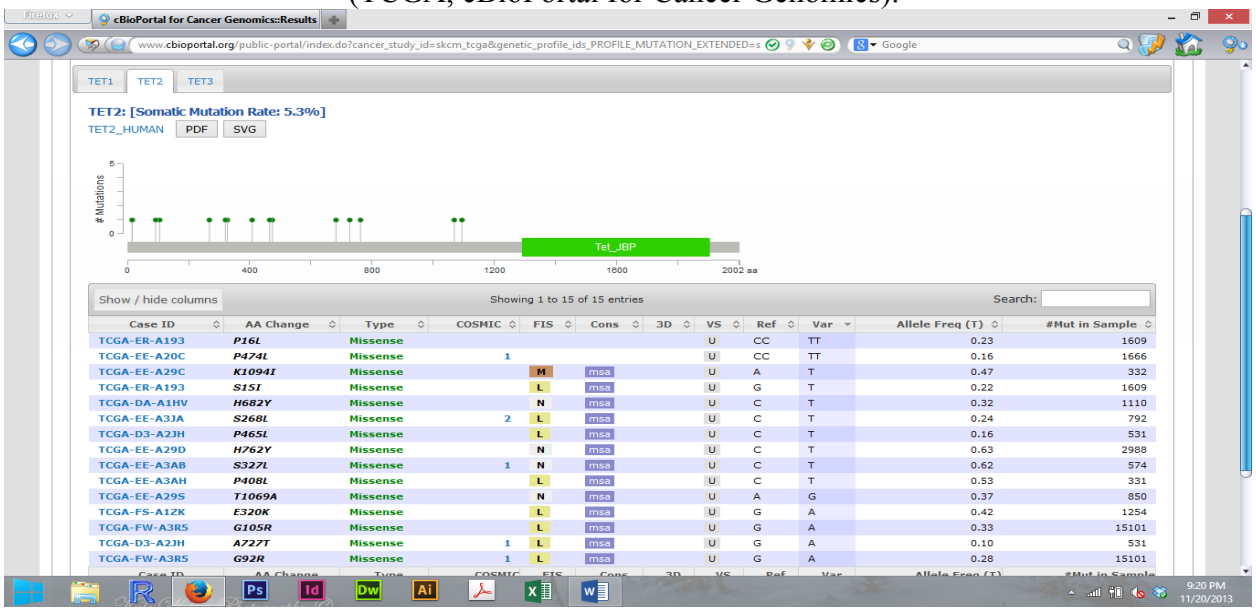

Figure 16b: TET2 mutations in skin cutaneous melanoma (TCGA, cBioPortal for Cancer Genomics).

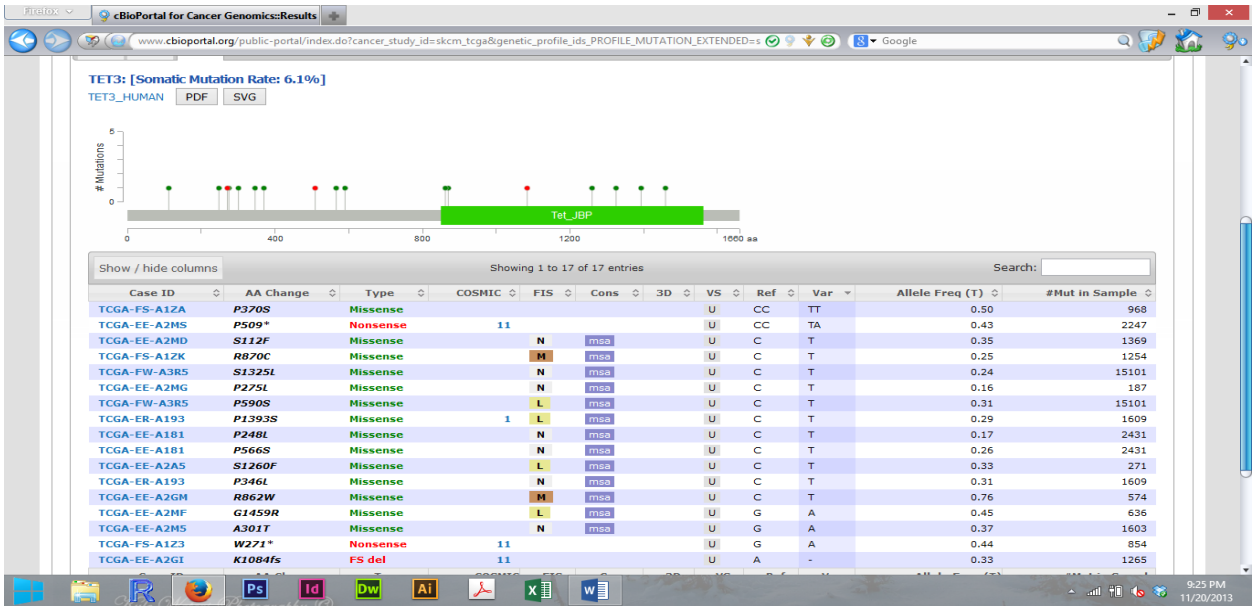

Figure 16c (Continued): TET3 mutations in skin cutaneous melanoma (TCGA, cBioPortal for Cancer Genomics).

More recently, as we have become interested in re-addressing our original question--whether UVB affects TET activity, we have begun looking at precisely quantifying 5hmC and downstream products (such as 5fC, 5caC), both as a function of TET2 overexpression and with time after irradiation. This is something that we have asked our mass spectrometry collaborators at UC Irvine (Prof. Y. Wang) to look at, as they recently published about their own neat standards for mass spectrometry quantification of 5hmC, 5fC, 5caC and other epigenetic markers (Liu *et al.*, 2013). One straightforward rationale for this study is that 5fC and 5caC are very newly discovered and barely examined epigenetic modifications, so any data we obtain would contribute to our understanding of the TET (specifically TET2) machinery. More importantly, we have another more ambitious interest in the UVB-DNA-TET2 interplay: The dynamic 5meC-5hmC seesaw (Figure 17a). Our interest has stemmed from our own previously inconclusive histology observations that UVB irradiation may alter 5hmC levels in primary cells (which

express high levels of 5hmC, similarly to our TET2 overexpressing cells). We only observed this phenomenon in a time course setting, which would support the notion that this was dependent on a cellular machinery, such as the TET pathway. Therefore our mass spectrometry study is being carried with respect to time post UVB treatment as well. As expected, TET2 overexpression alone dramatically increased 5hmC levels in melanoma cells by almost 9-fold (Figure 17b), in line with earlier dotblot (Figure 9a, Chapter 2) and other results (Lian *et al.*, 2012). Preliminary mass spectrometry results from S. Liu (Y. Wang's lab) indicate a 40% increase in genomic 5hmC levels (Figure 17b) in TET2 overexpressing melanoma cells within 24 hours of (broadspectrum) UVB treatment, accompanied by a 4% decrease in genomic 5meC levels (Figure 17c). If the relationship between 5hmC and 5meC were purely linear, we would expect only a 0.4% corresponding decrease in 5meC levels after 24 hours (initial, irradiated TET2+ cells with 0.0000559 5hmC/nucleoside and 0.023 5meC/dG = 0.00575 5meC/nucleoside corresponds to a 1 5hmC: 100 5meC ratio). We have sent more specimens to the mass spectrometry facility of our epigenetics collaborator Prof. Y. Shi, who picked up sample processing after our other collaborators decided to pursue other projects.

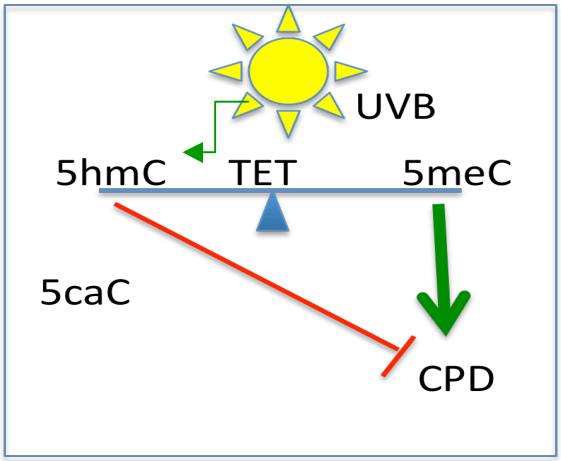

Figure 17a: The (hypothetical) dynamic 5meC-5hmC seesaw.

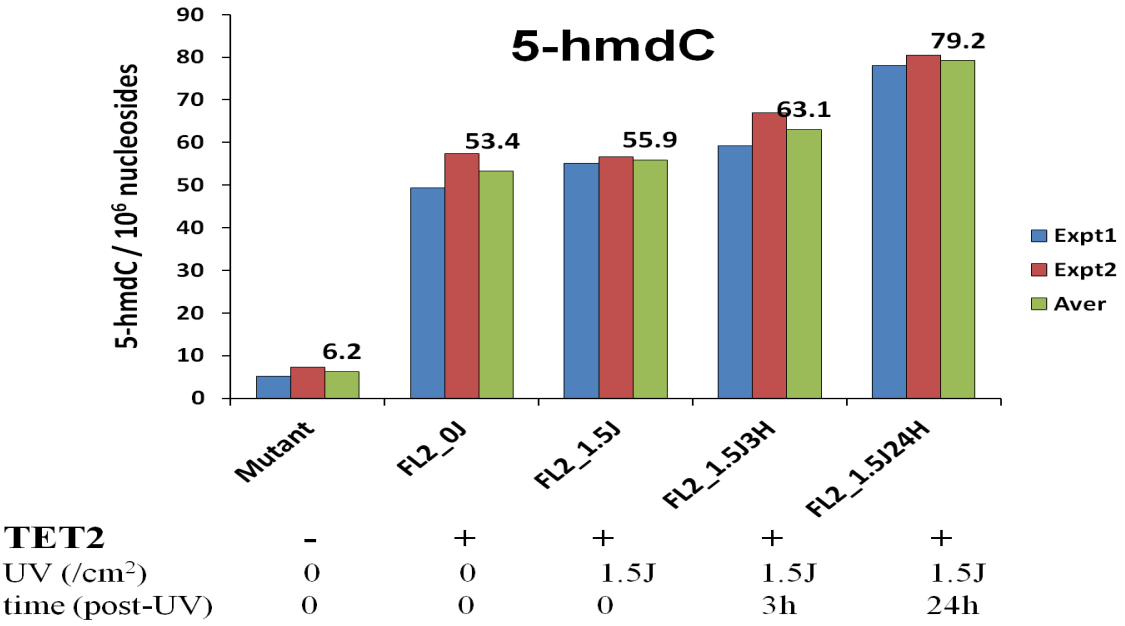

Figure 17b (Continued): 5hmC measurements in melanoma cells by mass spectrometry (technical duplicates, S. Liu and Y. Wang, UC Riverside).

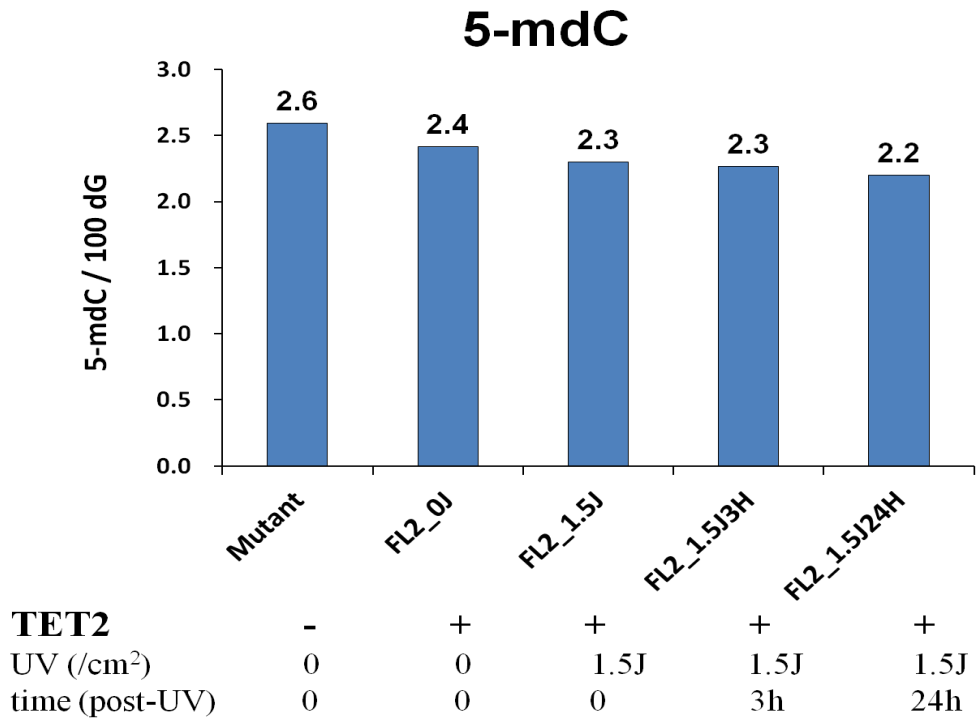

Figure 17c (Continued): 5meC measurements in melanoma cells by mass spectrometry (technical duplicates, S. Liu and Y. Wang, UC Riverside).

APPENDIX

Throughout my graduate research years, I worked on numerous projects that ultimately failed either due to technical limitations or ambiguous results. Two of them are worth mentioning here due to the interesting scientific questions that we posed.

Past Project #1 (Major Concern: UV crosslinking distorted histology data.)

(This project received NDSEG funding.)

EXECUTIVE SUMMARY

Because epithelial stem cells are thought to be the most likely targets of skin cancer initiation and tumor promotion (Morris, 2004), understanding the responses of the stratified epidermis to UV radiation, especially the effects of UVB on keratinocyte stem cells, has important implications for characterizing and utilizing skin stem cells, as well as for understanding and treating non-melanoma skin cancers.

RATIONALE

The normal cellular balance of life and death is regulated molecularly by the apoptosis machinery. Since UV radiation is a well-known trigger of the apoptotic cascade, there is considerable interest in understanding the apoptotic response of keratinocytes to UV-light. Current literature presents conflicting data on the UV-response of keratinocytes from different layers of the epidermis. I planned to characterize UV-induced apoptosis in keratinocytes, by first

identifying whether proliferative ability or differentiation status determines degree of sensitization or protection from UV-induced apoptosis. Subsequently, I investigated the mechanisms of this differential response to UV-light by examining the regulation of apoptosis machinery in keratinocytes. Furthermore, skin also exhibits robust regenerative capacity upon sun exposure, suggesting a subpopulation of cells with possibly stem-cell characteristics. Thus, I was also interested in isolating putative keratinocyte stem cells (KSC) from human skin in order to test if KSC's are resistant to UV induced apoptosis as a protective mechanism in normal skin. Finally, I planned to inject UV-treated keratinocytes of various subpopulations into immunocompromised mice as an *in vivo* model to explore long-term effects of UV irradiation on keratinocytes and as an extension to studying tumorigenesis of keratinocytes.

PRELIMINARY DATA

It is unclear which subpopulation(s) of human keratinocytes become apoptotic in response to UV radiation, since current literature presents conflicting data (Gniadecki *et al.*, 1997; Chaturvedi *et al.*, 1999; Tron *et al.*, 1998; Tron *et al.*, 1999). As a pilot study (see Figure A1), I used flow-cytometry-based propidium iodide/ annexin V staining of live cells to measure the apoptotic response 24hr after UV-irradiating (0, 20, or 40 mJ/cm^2) human foreskin keratinocytes. I repeated these experiments on human foreskin keratinocytes that were previously induced to differentiate via 72-hr incubation in high-calcium medium (1.2mM Ca^{++}). I also repeated the above experiments for the 48hr post-UV time point.

Preliminary flow cytometry data (see Figure A1) suggested that the basal, proliferating keratinocytes, which consist of mostly transiently amplifying (TA) cells, to be sensitive to UV-induced apoptosis, because higher fractions of Annexin V and PI-positive cells were observed by

flow cytometry when human foreskin keratinocytes were UV-treated for 24hr compared to non-UV-treated controls (left panel, Figure A1). For calcium-treated differentiating keratinocytes, the percentage of apoptotic cells remained constant across all doses of UV treatment and was comparable to control cells (right panel, Figure A1), suggesting that differentiated keratinocytes are resistant to UV-induced apoptosis. Controls (no dye or fluorescein-conjugated marker) confirm minimal background signals (top row, Figure A1). But the extent of differentiation was not measured in these in vitro assays, and thus further experiments were needed to validate the preliminary data.

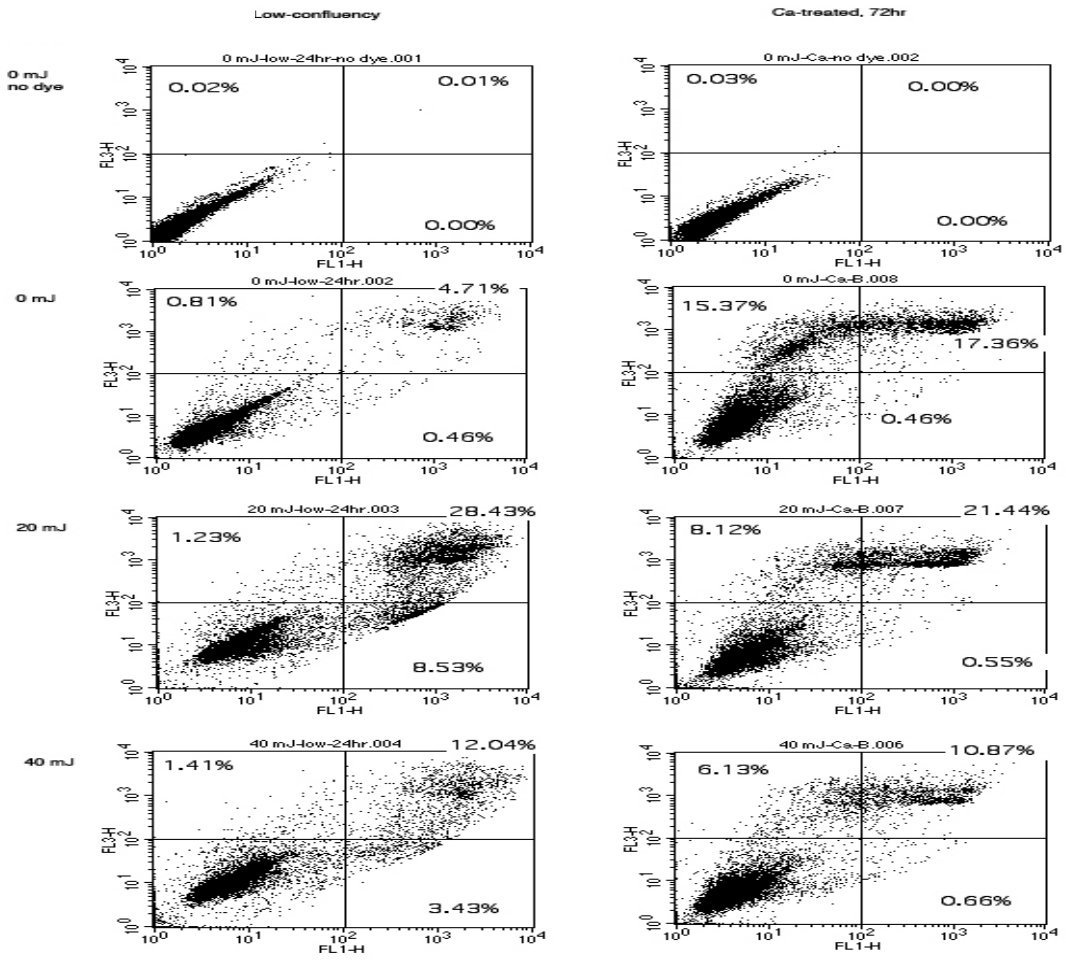

Figure A1: Annexin V/ PI live exclusion assay (FACS).

Furthermore, preliminary histology data suggested that a fraction of basal keratinocytes (possibly keratinocyte stem cells, KSCs) were protected from UV-induced apoptosis as well. Fresh human neonatal foreskin was UVB-irradiated at 250 mJ/cm^2, collected and processed after 5 hours, paraffin-embedded and stained for apoptosis via a fluorescent TUNEL assay (Figure A2). DAPI-counterstained nuclei (bottom row, Figure A2) highlight the layers of keratinocytes in human epidermis. While most keratinocytes in the UV-treated epidermis (and even dermis) labeled both DAPI- and TUNEL-positive (bright FITC signals, top row, Figure A2) to indicate abundant DNA fragmentation, some basal-layer keratinocytes only labeled DAPI-positive, suggesting that a fraction of basal keratinocytes may be resistant to UVB-induced apoptosis. Because keratinocyte stem cells probably reside in the epidermal basal layer of non-follicular skin (So *et al.*, 2004; Fuchs *et al.*, 2008), it is possible that, given the general resilience of stem cells, the UV-resistant basal keratinocytes correspond to a keratinocyte subpopulation with stem-like characteristics.

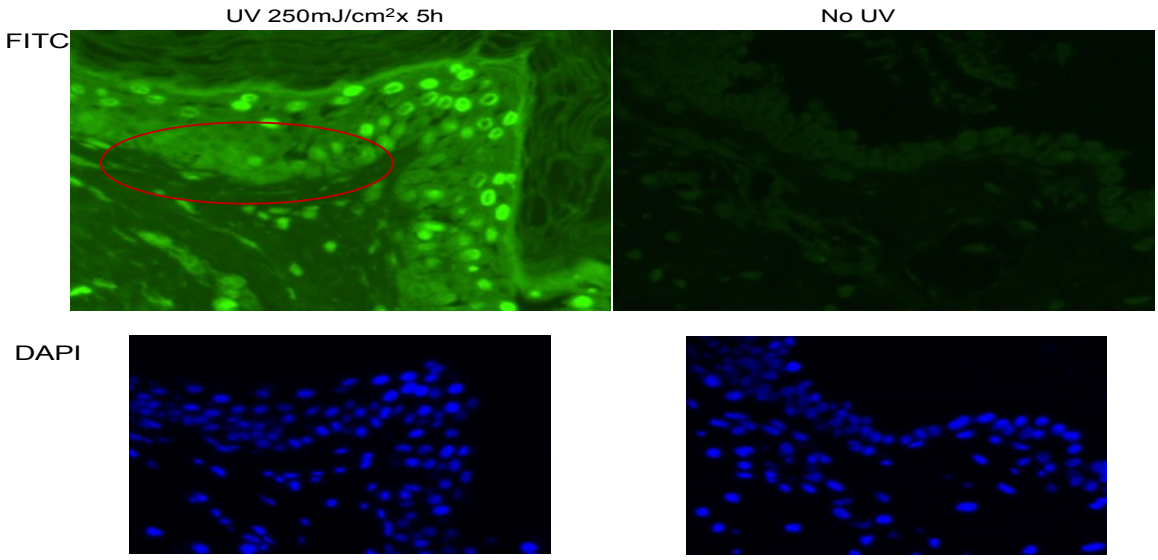

Figure A2: TUNEL staining.

Past Project #2 (Major Concern: Disagreement with collaborators on structure determination.)

(This project received F31 NRSA funding from the NIH.)

EXECUTIVE SUMMARY

Through studies on mouse skins and short oligonucleotides, we potentially discovered novel interstrand DNA adducts from UV radiation. UV radiation is known to cause DNA strand breaks and lesions. However, the UVB-signature CPD lesion is intrastrand, and in vitro interstrand experiments have used secondary crosslinking reagents such as mitomycin C. Our discovery of a novel cytosine interstrand (<CC>) adduct can be contributed to our unique Mass Tag Profiling methodology. Given the complexity (rigidity) of our hypothesized structure and the usually highly genotoxic nature of interstrand lesions, we investigated the impacts of our interstrand adducts on DNA damage and repair through *in vitro* repair-deficient cell models and *in vivo* skin samples, in addition to additional mass-spectrometry-based characterization studies.

RATIONALE

UV radiation from sunlight increases the risk of developing skin cancers, including malignant melanoma arising from the pigment-producing melanocytes in skin. However, the precise role of UV-induced DNA damage and repair in melanoma pathogenesis remains controversial. Many common melanoma mutations (such as BRAF somatic missense mutations) do not correspond to known UV signature mutations, and UV-signature CPD dimers and 6,4-photoproducts are absent in most melanomas (Kao et al., 2011).

Melanoma is the most dangerous type of skin cancer. With about 48,000 melanoma-related deaths reported worldwide every year, it is the leading cause of death from skin disease. However, while repeated exposure to UV radiation from sunlight is known to increase the risks

of developing all skin cancers by mutating the cellular DNA, currently known UVB-signature mutations from intrastrand pyrimidine dimers (CPD dimers) only account for the less deadly, non-melanoma skin cancers (BCC, SCC). The goal of this project was to identify and characterize novel UV-induced DNA lesions that may serve as new signature mutations for melanoma, in the hope that we may suggest new diagnostic tools for life-saving early detection and that new insights on melanoma pathogenesis may lead to more effective therapeutic interventions.

When UV radiation damages a cell, it mutates the cellular DNA with distinctive mutational patterns. Currently, the major known UVB lesions are pyrimidine dimers (Gale et al., Proc Natl Acad Sci U S A 1987), resulting in a four membered ring from covalent linkages of the carbon–carbon double bonds on adjacent pyrimidines. These cyclobutane-type pyrimidine dimers (CPDs) are quite mutagenic, especially in mammalian cells, initiating primary base substitutions in DNA. UVB induces cytosine to thymine transitions at the dipyrimidine sites, creating a UV-specific mutation signature that is ubiquitously observed in multiple organisms. UVB radiation produces most of the CPD photoproducts in mammalian skin compared to UVA, which comprises most sunlight radiation at the earth's surface; UVC is even more potent, but it is thought to be significantly screened out via the ozone layer.

However, CPD dimers are intrastrand lesions, much less toxic than their interstrand crosslinked counterparts. Among the early-known and widely-used chemotherapeutic agents, many such as cyclophosphamide and mitomycin C induce interstrand crosslinks (Deans and West, 2011). However, there is no evidence in current literature for direct UV-induced interstrand lesions. Since separation of the DNA double helix is essential for replication and transcription, interstrand lesions are deemed extremely toxic and usually irreversible. In

comparison, intrastrand crosslinks may be bypassed by some DNA polymerases, thus rendering them less toxic (Deans and West, 2011). Furthermore, repair of intrastrand crosslinks may be facilitated by the electronically favorable cyclic delocalization and resonance of the aromatic ring on DNA bases. While some information from the repair mechanisms of interstrand lesions is still missing, we know that interstrand lesion repair involves a complex coordination of nucleotide excision repair, homologous recombination and translesion synthesis, as well as the suppression of non-homologous end joining (Andreassen and Ren, 2009; Deans and West, 2011).

APPROACH

Aim 1: Identify new UV-induced lesions, especially the more genotoxic interstrand DNA lesions in order to provide significant insights for a causative link between UV radiation and melanoma.

Methodology 1: To pursue the first aim, we (a) used HPLC-MS/MS technology to identify UV-induced DNA adducts in various mouse models of pigmentation. For characterizing unique adducts, we used a novel Mass Tag Profiling methodology that has been recently developed by the Giese lab, our collaborators at the Northeastern University School of Pharmacy. I received mass spectrometry training and performed all experiments under supervision at their extensive HPLC and mass spectrometry facility. In brief, the Mass Tag Profiling methodology is as follows: Once DNA was extracted via Qiagen gravity-flow columns (based on prior experiments with cells and mouse skins, anion-exchange resin in QIAGEN-tips seemed more effective for purification and extraction of DNA from tissue samples than silica-membrane-based spin-columns), it was digested by to the nucleotide level, filtered, separated by HPLC, labeled with a

d0, d4, or d0/d4 benzoylhistamine tag, further filtered to remove excess tag, deposited with alpha-cyano matrix on a MALDI-plate, and finally analyzed through a MALDI-TOF machine. Due to the fact that our tagging labels only bound to free phosphates in a 1:1 stoichiometry, we (b) used variable tagging (heavy/light/mix) to determine inter- versus intrastrand-bonded nucleic acid adducts. Furthermore, we (c) tested UV-induction on a variety of oligonucleotides (combination of different dNTPs, methylation/other modifications of dNTPs) for structural insights into the DNA adducts. For a more comprehensive understanding of radiation-induced DNA lesions, we (d) measured the quantity of lesion induction under a range of wavelengths (UVA, UVB, gamma) and irradiation doses.

Hypothesis 1: We believe that heretofore unknown lesions—specifically, heretofore unknown novel interstrand DNA adducts—may represent a new UVB-signature lesion that can be linked to melanoma.

Preliminary Data 1: We utilized a new chemical approach to the analysis of genomic DNA after UV irradiation and discovered a relatively common occurrence of interstrand crosslinked DNA. Multiple follow-up studies have been carried out which have confirmed its existence, its intrastrand nature (both using the benzoylhistamine tag, and the oligos where the two crosslinked bases were only on opposite strands).

Initial screening for novel UV-induced DNA adducts was performed by HPLC-MS/MS on purified DNA from UV-irradiated skin of red-haired (e/e, frameshift mutation in Mc1r gene) or albino (c/c, mutation in the tyrosinase gene) K14-XPC(-/-) mice; controls were also provided (initial samples supplied by a fellow labmate, Dr. K. Robinson). In the UV-treated samples only, MassSpec profiling showed two novel, unique peaks (at 794.143 and 808.165 post-tagging) from

the HPLC fraction collected right after the Cytosine (C) peak (Figure A3). This indicated that these two structures, hereafter referred to as the "794" and "808" peaks, consist of a Cytosine-complex. Further fragmentation (MS/MS profiling) revealed that (1) the abundance of PO3 and PO4 in the MS/MS of the 808peak and 794 peak indicates that these are interstrand complexes (see "Potential Pitfalls and Strategies" below), also verified by oligonucleotide experiments with single cytosines; (2) MS and MS/MS profiling suggests that the complexes each consist of 2 cytosines; (3) position of complexes on the UV-spectrographs (relative too position of Cytosine-peak) further suggests 2-cytosine-adducts; (4) fragmentation of the complexes at their loss-of-tag m/z precursor ratios is in accordance with the above observations, suggesting that this is not an artifact of the MassTag Profiling methodology; (5) both complexes were abundantly present in e/e and c/c UVB-irradiated DNA (on the order of 30ppm, about 1/5 the level of CPD induction), but completely absent from unirradiated controls as well as from UVA-irradiations, suggesting a UVB-only adduct induction.

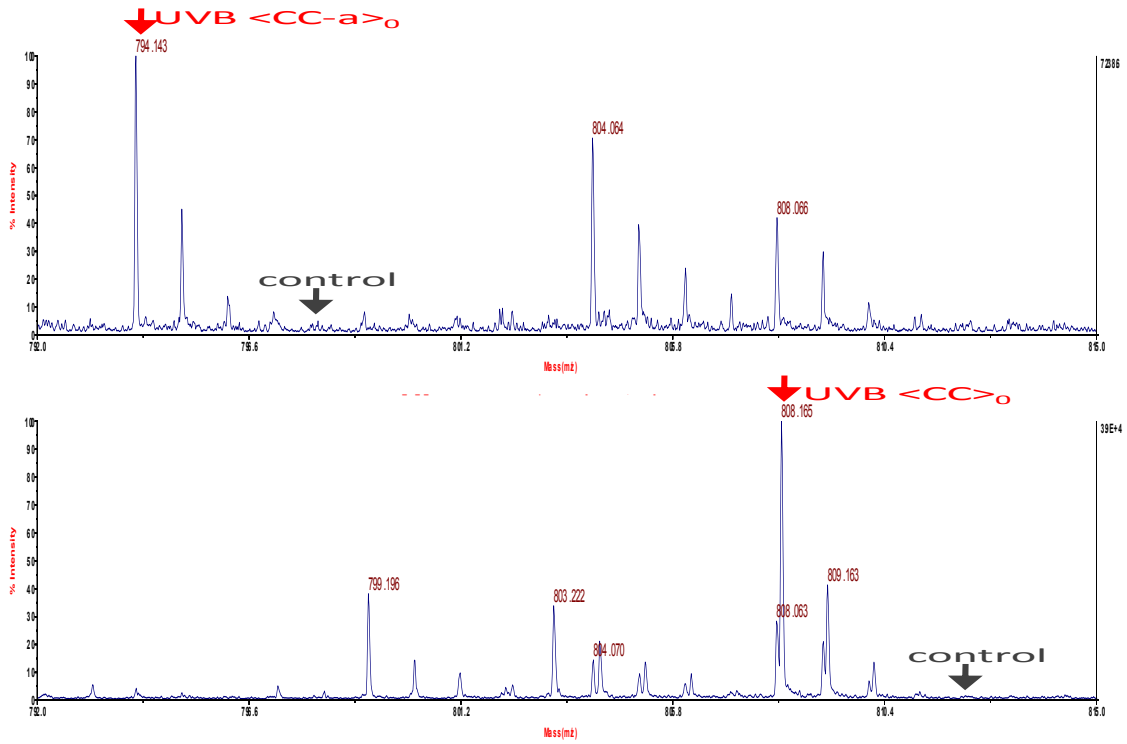

Figure A3: Induction of interstrand cytosine adducts by UVB irradiation (on red (e/e) mouse skin); d_0 tag = UVB; d_4 tag= control.

Anticipated Results 1: With the help of newly developed Mass Tag Profiling methodology with our collaborators, initial HPLC-MS/MS profiles from UVB-irradiated mouse skins led us to suspect that we found unique UV-induced interstrand adducts *in vivo*, which have not been previously identified/ reported in literature. We expected re-testing of DNA from replicate skin samples and from skin cells in culture to concur with the above data. We expected further experiments on oligonucleotides to reveal clues about preferences of adduct induction (e.g., tight GCGCGC sequences might be too bulky for efficient induction, as might certain base modifications), which would enable us to propose mechanisms for UV-induced adduct formation. Furthermore, given the time- and resource-consuming nature of mass spectrometry preparations/experiments, we expected to develop molecular biology assays for distinguishing our novel cytosine interstrand adducts from other lesions (e.g. by fluorescently-tagged

denaturing gel shift assays that would distinguish between inter- versus intrastrand adducts. Given the usually highly genotoxic nature of interstrand lesions, our findings could have a significant impact on our understanding of UV-induced DNA damage and cellular repair.

Potential Pitfalls and Strategies:

Our 808 and 794 peaks have unique MS signatures, thus reducing the likelihood of false positives and helping to ensure the accuracy of our abundance calculations.

MS/MS fragmentation reveals abundant free phosphates in the tagged adduct, which is only feasible if the adduct is interstrand. Our unique Mass Tag Profiling methodology, with a benzyolhistamine tag on any free phosphate, enabled us to uniquely distinguish between inter- and intrastrand crosslinked complexes.

Our reciprocal labeling with d_0, d_4, d_0/d_4 tags enabled us to doubly confirm the identity of any peaks of interest on a mass spectrometry profile. Loss-of-tag profiling then let us rule out artificial peaks from the alpha-cyano matrix.

We always incorporated a 575 internal standard uniformly into our MALDI depositions; furthermore, we used the widely-known UVB-induced CPD dimer as another standard for measuring and quantifying peak intensities into parts per million abundance values.

To help ensure replicable HPLC fraction collections, we thoroughly flushed the instrument with 100% acetonitrile and run a blank sample at 0.05% acetonitrile to check for trace peaks on the UV spectrograph. All collections started and ended at a predetermined threshold intensity. We re-run samples if the spectrographs do not line up. Furthermore, we deposited at least 400 spots per fraction on the MALDI plate to avoid any missed signals.

To prevent any heat-induced artificiality in our oligo work, we performed oligo irradiations on an ice bucket and pause every 20min. Thermometer readings indicated no increase in temperatures during irradiations, and the volume of samples remained consistent (minimal evaporation: 1ul/100ul loss after 1 hour irradiation=3000mJ/cm2 UVB). Furthermore, mass spectrometry profiles of UV-irradiated oligos under ice and at room temperature showed the same 808 peak profiling.

Aim 2: Characterize the novel interstrand lesions and their repair kinetics in order to identify new UV-signature mutations for illuminating molecular mechanisms behind melanoma pathogenesis.

Methodology 2: To pursue the second aim, we (a) used organic synthesis to validate our hypothesized structures; with well-developed structure hypotheses, we could better develop diagnostic tools for studying novel adducts. To accomplish this task, we planned to use boronic acid conjugates of cytosine and cytosine halides for a Suzuki coupling reaction to give the regioisomers of our hypothesized structure (Figure A4).

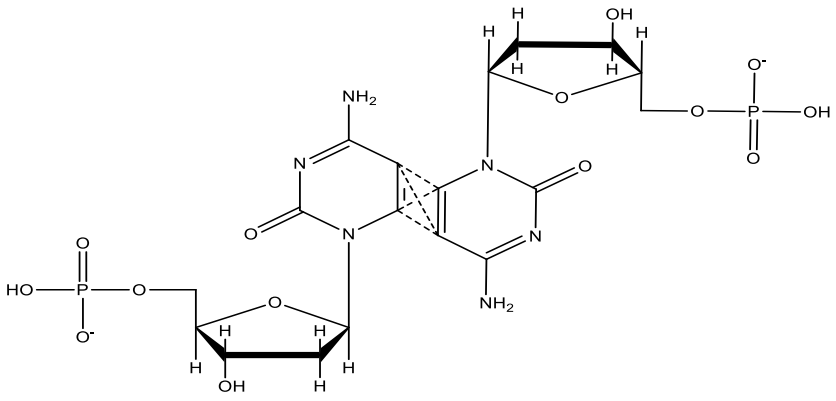

Figure A4: Hypothesized structure of interstrand adduct.

(b) Together with flow-cytometry-based studies of repair kinetics and modified shuttle vector mutagenesis assays, we could identify the signature mutations of these novel UV-induced adducts, which (as suggested by preliminary analyses) could be aligned to genomic mutation patterns from melanoma databanks, thus helping us understand UV-induced melanoma pathogenesis. More specifically, flow-cytometry-based studies of repair kinetics would be performed by harvesting primary skin cells (keratinocytes) from culture, then sorted into live versus dead populations, and quantified for the amount of adducts pre- and post-irradiation at various timepoints via HPLC-MS/MS to establish the efficiency/rate of repair.

(c) Furthermore, we aim to identify key players in the repair of interstrand lesions via studying DNA repair-deficient cell models.

(d) We could adapt current shuttle vector mutagenesis assays as follows: After UVB-irradiating GFP plasmids, we would remove other photoproducts via CPD- and 6,4-photolyases, transfect into skin cells, track and extract DNA post-repair, sequence/analyze original adduct sites to determine mutations. We would compare these results with bioinformatical analysis for mutation hotspots in melanomas through a genomics collaboration with the Broad Institute, with the hope of linking prominent mutations in melanomas (when matched to normal) to erroneous repair of our UVB-induced interstrand crossslinked adducts, thus revealing a new UVB-signature mutation(s) that is unique to melanomas.

Hypothesis 2: Due to the genotoxity of interstrand lesions, we believed repair of our interstrand adducts to be error-prone (new UVB-signature mutation) and/or inefficient (induced cell death). We strove to demonstrate that cellular repair of novel interstrand DNA lesions leads to cellular

DNA mutations (different from known photoproducts) that show high incidence in melanomas but not other non-skin cancers (such as ovarian, colorectal).

Preliminary Data 2: Initial repair kinetics experiments on mice (sacrificing and extracting UVB-irradiated mice at various timepoints) have indicated that most of the UVB-induced interstrand cytosine adducts disappear within 24hr (Figure A5). In our very recently formed genomics collaboration with the Broad Institute, we examined mutation patterns for melanomas (matched to normal) and ovarian cancer (matched to normal as well). We focused on trinucleotide contexts where any subsequent mutations could not be explained by 6.4-photoproducts or CPD dimers (that is, pyrimidine-dimer-independent context would be of purine-Cytosine-purine type). We found 2 groups of "hot" mutations (i.e., high incidence in melanomas), as follows: 1. C->T transitions (even in purine-Cytosine-purine context, thus not attributed to CPD, 6,4-photoproducts); 2. C->G transversions. Due to the frequency of natural C->T transitions at CpG islands, we chose to focus on the 2nd group of "hot" mutations in melanomas, the C->G transversions (which, one could argue, would constitute a more significant mutation solely due to the large structural substitution and electronic repulsions between the guanine bases). One of our goals was to link these C->G mutations in melanomas to erroneous repair of our UVB-induced interstrand crosslinked cytosine lesions.

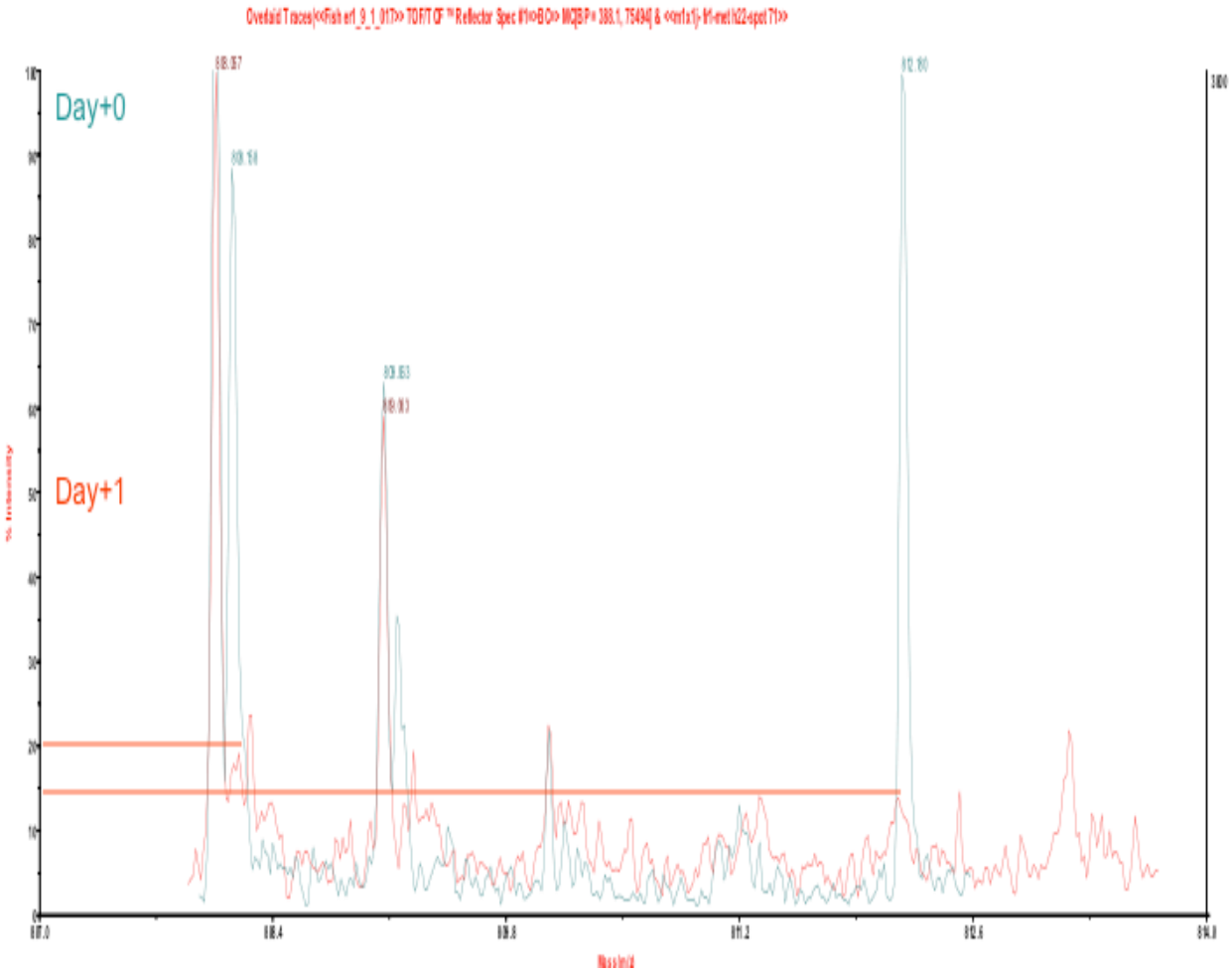

Figure A5: Quantity of UVB-induced interstrand cytosine adducts (peaks indicated by orange horizontal lines) significantly declines by 24hr (compare heights of overlapping peaks).

Anticipated Results 2: We expected the mass spectrometry profiles of synthesized adducts to match that from our *in vivo* mouse experiments (and oligo experiments), thus further supporting our hypothesized adduct structure (Figure A4). Together with flow-cytometry-based studies of repair kinetics and modified shuttle vector mutagenesis assays, we could identify the signature mutations of these novel UV-induced adducts, which (as suggested by preliminary analyses) could be aligned to genomic mutation patterns from melanoma databanks, thus helping us understand UV-induced melanoma pathogenesis.

Potential Pitfalls and Strategies:

We were aware that our results are only as good as the technical limitations of our instruments. Thus, at all steps, especially repair experiments that were measuring declining quantities, we aimed to magnify our signals via GFP/fluorescent/double-labeling/other tagging/internal controls.

We recently became aware that the starting materials for our proposed organic synthesis experiment (for structural characterization) may not be available due to thermodynamic instability of boronic-acid-conjugates of cytosine. However, we could circumvent this problem by performing the Suzuki coupling reaction on uracil instead. We would then perform deamination of our interstrand cytosine adducts isolated from *in vivo* samples (via bisulfite treatment) to give equivalent uracil-interstrand-adducts, run Mass Tag Profiling, and compare with mass spec profiling from synthesized uracil adducts to validate our hypothesized adduct structures.

LITERATURE CITED

Alberts, B., Johnson, A., Lewis, J., Raff, M., Roberts, K., and Walter, P. (2002). Molecular Biology of The Cell (New York: Garland Science).

Alonso L, Fuchs E. (2003). Stem cells of the skin epithelium. Proc Natl Acad Sci U S A. *100* Suppl 1:11830-5.

Andreassen PR, Ren K. Fanconi anemia proteins, DNA interstrand crosslink repair pathways, and cancer therapy. (2009). Curr Cancer Drug Targets. *9*, 101-17.

Booth MJ, Branco MR, Ficz G, Oxley D, Krueger F, Reik W, Balasubramanian S. (2012). Quantitative sequencing of 5-methylcytosine and 5-hydroxymethylcytosine at single-base resolution. Science. *336*, 934-7.

Brash DE, Seetharam S, Kraemer KH, Seidman MM, Bredberg A. (1987). Photoproduct frequency is not the major determinant of UV base substitution hot spots or cold spots in human cells. Proc Natl Acad Sci U S A. *84*, 3782-6.

Brash D, Rudolph J, Simon J, Lin A, McKenna G, Baden H, Halperin A, Pontén J. (1991). A role for sunlight in skin cancer: UV-induced p53 mutations in squamous cell carcinoma. Proc Natl Acad Sci U S A. *88*, 10124-8.

Cannistraro VJ, Taylor J-S. (2009). Acceleration of 5-methylcytosine deamination in cyclobutane dimers by G and its implications for UV-induced C-to-T mutation hotspots. J Mol Biol. *392*, 1145-57.

Chaturvedi V, Qin J, Denning M, Choubey D, Diaz M, Nickoloff B. (1999). Apoptosis in proliferating, senescent, and immortalized keratinocytes. J Biol Chem. *274*, 23358-67.

Cleaver J, Crowley E. (2002). UV damage, DNA repair and skin carcinogenesis. Front Biosci. *7*, d1024-43.

Cotton J, Spandau DF. (1997). Ultraviolet B-radiation dose influences the induction of apoptosis and p53 in human keratinocytes. Radiat Res. *147*, 148-55.

Deans AJ, West SC. DNA interstrand crosslink repair and cancer. (2011). Nat Rev Cancer. *11*, 467-80.

Douki T. (2006). Low ionic strength reduces cytosine photoreactivity in UVC-irradiated isolated DNA. Photochem Photobiol Sci. 5, 1045-51.

Douki T, Cadet J. (1994). Formation of cyclobutane dimers and (6-4) photoproducts upon far-UV photolysis of 5-methylcytosine-containing dinucleotide monophosphates. Biochemistry. *33*, 11942-50.

Douki T, Court M, Sauvaigo S, Odin F, Cadet J. (2000). Formation of the main UV-induced thymine dimeric lesions within isolated and cellular DNA as measured by high performance liquid chromatography-tandem mass spectrometry. J Biol Chem. *275*, 11678-85.

Fears TR, Bird CC, Guerry D 4th, Sagebiel RW, Gail MH, Elder DE, Halpern A, Holly EA, Hartge P, Tucker MA. (2002). Average midrange ultraviolet radiation flux and time outdoors predict melanoma risk. Cancer Res. *62*, 3992-6.

Franklin WA, Doetsch PW, Haseltine WA. (1985). Structural determination of the ultraviolet light-induced thymine-cytosine pyrimidine-pyrimidone (6-4) photoproduct. Nucleic Acids Res. *13*, 5317-25.

Fuchs E. (2008). Skin stem cells: rising to the surface. J Cell Biol.*180*, 273-84.

Gale JM, Nissen KA, Smerdon MJ. (1987). UV-induced formation of pyrimidine dimers in nucleosome core DNA is strongly modulated with a period of 10.3 bases. Proc Natl Acad Sci U S A. *84*, 6644-8.

Gambichler T, Sand M, Skrygan M. (2013). Loss of 5-hydroxymethylcytosine and ten-eleven translocation 2 protein expression in malignant melanoma. Melanoma Res. *23*, 218-20.

Globisch D, Münzel M, Müller M, Michalakis S, Wagner M, Koch S, Brückl T, Biel M, Carell T. (2010). Tissue distribution of 5-hydroxymethylcytosine and search for active demethylation intermediates. PLoS One. *5*, e15367.

Gniadecki R, Hansen M, Wulf H. (1997). Two pathways for induction of apoptosis by ultraviolet radiation in cultured human keratinocytes. J Invest Dermatol. *109*, 163-9.

Gong Z, Zhu JK. (2011). Active DNA demethylation by oxidation and repair. Cell Res. *21*, 1649-51.

Häder DP, Sinha RP. (2005). Solar ultraviolet radiation-induced DNA damage in aquatic organisms: potential environmental impact. Mutat Res. *571*, 221-33.

Ito S, D'Alessio AC, Taranova OV, Hong K, Sowers LC, Zhang Y. (2010). Role of Tet proteins in 5mC to 5hmC conversion, ES-cell self-renewal and inner cell mass specification. Nature. *466*, 1129-33.

Jäwert F, Hasséus B, Kjeller G, Magnusson B, Sand L, Larsson L. (2013). Loss of 5-hydroxymethylcytosine and TET2 in oral squamous cell carcinoma. Anticancer Res. *33*, 4325-8.

Jin SG, Jiang Y, Qiu R, Rauch TA, Wang Y, Schackert G, Krex D, Lu Q, Pfeifer GP. (2011). 5-Hydroxymethylcytosine is strongly depleted in human cancers but its levels do not correlate with IDH1 mutations. Cancer Res. *71*, 7360-5.

Kan LS, Voituriez L, Cadet J. (1992). The Dewar valence isomer of the (6-4) photoadduct of thymidylyl-(3'-5')-thymidine monophosphate: formation, alkaline lability and conformational properties. J Photochem Photobiol B. *12*, 339-57.

Kao WH, Riker AI, Kushwaha DS, Ng K, Enkemann SA, Jove R, Buettner R, Zinn PO, Sánchez NP, Villa JL, D'Andrea AD, Sánchez JL, Kennedy RD, Chen CC, Matta JL. (2011). Upregulation of Fanconi anemia DNA repair genes in melanoma compared with non-melanoma skin cancer. J Invest Dermatol. *131*, 2139-42.

Keyse SM, Amaudruz F, Tyrrell RM. (1988). Determination of the spectrum of mutations induced by defined-wavelength solar UVB (313-nm) radiation in mammalian cells by use of a shuttle vector. Mol Cell Biol. *8*, 5425-31.

Kim JK, Choi BS. (1995). The solution structure of DNA duplex-decamer containing the (6-4) photoproduct of thymidylyl(3'-->5')thymidine by NMR and relaxation matrix refinement. Eur J Biochem. *228*, 849-54.

Kim SI, Jin SG, Pfeifer GP. (2013). Formation of cyclobutane pyrimidine dimers at dipyrimidines containing 5-hydroxymethylcytosine. Photochem Photobiol Sci. *12*, 1409-15.

Kinney SR, Pradhan S. (2013). Ten eleven translocation enzymes and 5-hydroxymethylation in mammalian development and cancer. Adv Exp Med Biol. *754*, 57-79.

Koh KP, Yabuuchi A, Rao S, Huang Y, Cunniff K, Nardone J, Laiho A, Tahiliani M, Sommer CA, Mostoslavsky G, Lahesmaa R, Orkin SH, Rodig SJ, Daley GQ, Rao A. (2011). Tet1 and Tet2 regulate 5-hydroxymethylcytosine production and cell lineage specification in mouse embryonic stem cells. Cell Stem Cell. *8*, 200-13.

Kriaucionis S, Heintz N. (2009). The nuclear DNA base 5-hydroxymethylcytosine is present in Purkinje neurons and the brain. Science. *324*, 929-30.

LeClerc JE, Borden A, Lawrence CW. (1991). The thymine-thymine pyrimidine-pyrimidone(6-4) ultraviolet light photoproduct is highly mutagenic and specifically induces 3' thymine-to-cytosine transitions in Escherichia coli. Proc Natl Acad Sci U S A. *88*, 9685-9.

Lee DH, Pfeifer GP. (2003). Deamination of 5-methylcytosines within cyclobutane pyrimidine dimers is an important component of UVB mutagenesis. J Biol Chem. *278*, 10314-21.

Lee JH, Bae SH, Choi BS. (2000). The Dewar photoproduct of thymidylyl(3'-->5')- thymidine (Dewar product) exhibits mutagenic behavior in accordance with the "A rule". Proc Natl Acad Sci U S A. *97*, 4591-6.

Lee JH, Hwang GS, Choi BS. (1999). Solution structure of a DNA decamer duplex containing the stable 3' T.G base pair of the pyrimidine(6-4)pyrimidone photoproduct [(6-4) adduct]: implications for the highly specific 3' T --> C transition of the (6-4) adduct. Proc.Natl.Acad.Sci.USA *96,* 6632-6636.

Lian CG, Xu Y, Ceol C, Wu F, Larson A, Dresser K, Xu W, Tan L, Hu Y, Zhan Q, Lee CW, Hu D, Lian BQ, Kleffel S, Yang Y, Neiswender J, Khorasani AJ, Fang R, Lezcano C, Duncan LM, Scolyer RA, Thompson JF, Kakavand H, Houvras Y, Zon LI, Mihm MC Jr, Kaiser UB, Schatton T, Woda BA, Murphy GF, Shi YG. (2012). Loss of 5-hydroxymethylcytosine is an epigenetic hallmark of melanoma. Cell. *150*, 1135-46.

Lippke JA, Gordon LK, Brash DE, Haseltine WA. (1981). Distribution of UV light-induced damage in a defined sequence of human DNA: detection of alkaline-sensitive lesions at pyrimidine nucleoside-cytidine sequences. Proc Natl Acad Sci U S A. *78*, 3388-92.

Liu JJ, Fisher DE. (2010). Lighting a path to pigmentation: mechanisms of MITF induction by UV. Pigment Cell Melanoma Res. *6*, 741-5.

Liu S, Wang J, Su Y, Guerrero C, Zeng Y, Mitra D, Brooks PJ, Fisher DE, Song H, Wang Y. (2013). Quantitative assessment of Tet-induced oxidation products of 5-methylcytosine in cellular and tissue DNA. Nucleic Acids Res. *41*, 6421-9.

Mitchell DL, Haipek CA, Clarkson JM. (1985). (6-4)Photoproducts are removed from the DNA of UV-irradiated mammalian cells more efficiently than cyclobutane pyrimidine dimers. Mutat Res. *143*, 109-12.

Mitchell DL, Jen J, Cleaver JE. (1992). Sequence specificity of cyclobutane pyrimidine dimers in DNA treated with solar (ultraviolet B) radiation. Nucleic Acids Res. *20*, 225-9.

Mitchell DL. (2000). Effects of cytosine methylation on pyrimidine dimer formation in DNA. Photochem Photobiol. *71*, 162-5.

Miyamura Y, Coelho SG, Wolber R, Miller SA, Wakamatsu K, Zmudzka BZ, Ito S, Smuda C, Passeron T, Choi W, Batzer J, Yamaguchi Y, Beer JZ, Hearing VJ. (2007). Regulation of human skin pigmentation and responses to ultraviolet radiation. Pigment Cell Res. *20*, 2-13.

Morris RJ. (2004). A perspective on keratinocyte stem cells as targets for skin carcinogenesis. Differentiation. 72, 381-6.

Münzel M, Globisch D, Carell T. (2011). 5-Hydroxymethylcytosine, the sixth base of the genome. Angew Chem Int Ed Engl. *50*, 6460-8.

Nestor C, Ruzov A, Meehan R, Dunican D. (2010). Enzymatic approaches and bisulfite sequencing cannot distinguish between 5-methylcytosine and 5-hydroxymethylcytosine in DNA. Biotechniques. *4*, 317-9.

Otoshi E, Yagi T, Mori T, Matsunaga T, Nikaido O, Kim ST, Hitomi K, Ikenaga M, Todo T. (2000). Respective roles of cyclobutane pyrimidine dimers, (6-4)photoproducts, and minor

photoproducts in ultraviolet mutagenesis of repair-deficient xeroderm pigmentosum A cells. Cancer Res. *60*, 1729-35.

Pastor WA, Pape UJ, Huang Y, Henderson HR, Lister R, Ko M, McLoughlin EM, Brudno Y, Mahapatra S, Kapranov P, Tahiliani M, Daley GQ, Liu XS, Ecker JR, Milos PM, Agarwal S, Rao A. (2011). Genome-wide mapping of 5-hydroxymethylcytosine in embryonic stem cells. Nature. *473*, 394-7.

Paz M, Ferrari A, Weill F, Leoni J, Maglio D. (2008). Time-course evaluation and treatment of skin inflammatory immune response after ultraviolet B irradiation. Cytokine. *44*, 70-7.

Pettersen EF, Goddard TD, Huang CC, Couch GS, Greenblatt DM, Meng EC, Ferrin TE. (2004). UCSF Chimera--a visualization system for exploratory research and analysis. *J Comput Chem. 13*, 1605-12.

Rochette PJ, Lacoste S, Therrien JP, Bastien N, Brash DE, Drouin R. (2009). Influence of cytosine methylation on ultraviolet-induced cyclobutane pyrimidine dimer formation in genomic DNA. Mutat Res. *665*, 7-13.

Shen L, Wu H, Diep D, Yamaguchi S, D'Alessio AC, Fung HL, Zhang K, Zhang Y. (2013). Genome-wide analysis reveals TET- and TDG-dependent 5-methylcytosine oxidation dynamics. Cell. *153*, 692-706.

So P, Epstein E Jr. (2004). Adult stem cells: capturing youth from a bulge? Trends Biotechnol. *22*, 493-6.

Song CX, He C. (2013). Potential functional roles of DNA demethylation intermediates. Trends Biochem Sci. *38*, 480-4.

Song CX, Szulwach KE, Dai Q, Fu Y, Mao SQ, Lin L, Street C, Li Y, Poidevin M, Wu H, Gao J, Liu P, Li L, Xu GL, Jin P, He C. (2013). Genome-wide profiling of 5-formylcytosine reveals its roles in epigenetic priming. Cell. *153*, 678-91.

Szekeres G, Siklós P, Nagy L, Jelinek L. (1976). Thermal dimerization of cyclopentadiene and its reaction with isoprene. (Presented by Prof. Dr. I. Szebényi).

Tahiliani M, Koh KP, Shen Y, Pastor WA, Bandukwala H, Brudno Y, Agarwal S, Iyer LM, Liu DR, Aravind L, Rao A. (2009). Conversion of 5-methylcytosine to 5-hydroxymethylcytosine in mammalian DNA by MLL partner TET1. Science. *324*, 930-5.

Tan L, Shi YG. (2012). Tet family proteins and 5-hydroxymethylcytosine in development and disease. Development. *139*, 1895-902.

Tommasi S, Denissenko MF, Pfeifer GP. (1997). Sunlight induces pyrimidine dimers preferentially at 5-methylcytosine bases. Cancer Res. *57*, 4727-30.

Tornaletti S, Pfeifer GP. (1995). Complete and tissue-independent methylation of CpG sites in the p53 gene: implications for mutations in human cancers. Oncogene. *10*, 1493-9.

Tran T, Schulman J, Fisher D. (2008). UV and pigmentation: molecular mechanisms and social controversies. Pigment Cell Melanoma Res. *21*, 509-16.

Tron VA, Trotter MJ, Tang L, Krajewska M, Reed JC, Ho VC, Li G. (1998). p53-regulated apoptosis is differentiation dependent in ultraviolet B-irradiated mouse keratinocytes. Am J Pathol. *153*, 579-85.

Tron VA, Li G, Ho V, Trotter MJ. (1999). Ultraviolet radiation-induced p53 responses in the epidermis are differentiation-dependent. J Cutan Med Surg. *3*, 280-3.

Witkin EM. (1975). Persistence and decay of thermoinducible error-prone repair activity in nonfilamentous derivatives of tif-1, Escherichia coli B/r: the timing of some critical events in ultraviolet mutagenesis. Mol Gen Genet. *142*, 87-103.

Wu YC, Ling ZQ. (2014). The role of TET family proteins and 5-hydroxymethylcytosine in human tumors. Histol Histopathol. [Epub ahead of print] PubMed PMID: 24585390.

Wyatt GR, Cohen SS. (1952). A new pyrimidine base from bacteriophage nucleic acids. Nature. *170*, 1072-1073.

Yamaguchi Y, Hearing VJ. (2009). Physiological factors that regulate skin pigmentation. Biofactors. *35*, 193-9.

Yamaguchi Y, Takahashi K, Zmudzka BZ, Kornhauser A, Miller SA, Tadokoro T, Berens W, Beer JZ, Hearing VJ. (2006). Human skin responses to UV radiation: pigment in the upper epidermis protects against DNA damage in the lower epidermis and facilitates apoptosis. FASEB J. *20*, 1486-8.

Yamamoto J, Hitomi K, Todo T, Iwai S. (2006). Synthesis of oligonucleotides containing the Dewar valence isomer of the (6-4) photoproduct and their application to (6-4) photolyase studies. Nucleic Acids Symp Ser (Oxf). *50*, 61-2.

Yang H, Liu Y, Bai F, Zhang JY, Ma SH, Liu J, Xu ZD, Zhu HG, Ling ZQ, Ye D, Guan KL, Xiong Y. (2013). Tumor development is associated with decrease of TET gene expression and 5-methylcytosine hydroxylation. Oncogene. *32*, 663-9.

You YH, Li C, Pfeifer GP. (1999). Involvement of 5-methylcytosine in sunlight-induced mutagenesis. J Mol Biol. *293*, 493-503.

You YH, Pfeifer GP. (2001). Similarities in sunlight-induced mutational spectra of CpG-methylated transgenes and the p53 gene in skin cancer point to an important role of 5-methylcytosine residues in solar UV mutagenesis. J Mol Biol. *305*, 389-99.